5-2021

Synthesis, characterization, and reactivity of organometallic complexes for catalytic carbon-hydrogen bond activation

Sophia Neglia
University of Tennessee at Chattanooga, lkp711@mocs.utc.edu

Synthesis, Characterization, and Reactivity of Organometallic Complexes for Catalytic Carbon-Hydrogen Bond Activation

Sophia Elizabeth Neglia

Departmental Honors Thesis
University of Tennessee at Chattanooga
Department of Chemistry and Physics

Examination Date:
April 12th, 2021

John P. Lee
Professor of Chemistry
Thesis Director

Jared A. Pienkos
Professor of Chemistry
Department Examiner

Titus V. Albu
Professor of Chemistry
Department Examiner

Abstract

Styrene can be produced directly from benzene and ethylene through an atom economical oxidative hydroarylation process. In this process, an electrophilic homogeneous transition metal catalyst activates the C-H bond in benzene. I propose to explore this reaction in two fronts: 1) the synthesis of electron-poor *trans*-spanning bidentate pyridine ligands and 2) the computational study of pyridine-functionalized bidentate diimines. The *trans*-spanning ligand will utilize either a Ru(II) or Co(III) metallohinge with *cis*-coordinated 2-ethynylpyridine ligands. The complex [(*p*-cym)Ru(PMe_3)(C_2-2-py)$_2$] (**1**) where (*p*-cym = *para*-cymene and C_2-2-py = 2-ethynylpyridine) can be prepared from (*p*-cym)Ru(PMe_3)(Cl)$_2$ and HC_2-2-py in the presence of lithium bis(trimethylsilyl)amide (LiHMDS). Complex **1** has been characterized by ^{1}H and ^{31}P NMR spectroscopy where the ^{31}P NMR chemical shift at 15.2 ppm confirmed when the alkynyl-pyridine ligands were attached, and the ^{1}H NMR showed mirror symmetry which is consistent with the proposed complex. Pd(II) acetate was attempted to coordinate to **1** in a *trans* fashion to make [(*p*-cym)Ru(PMe_3)(C_2-2-py)$_2$Pd(OAc)$_2$], however this gave inconclusive NMR results. This reaction was extended to the electron-poor Co(III) to prepare [Cp*Co(PMe_3)(C_2-2-py)$_2$] (**2**) where (Cp* = pentamethyl cyclopentadienyl anion) from [Cp*Co(PMe_3)(I)$_2$]. Additional ligand analysis involved density functional theory (DFT) calculations using the B3LYP functional in Gaussian 16 software to determine the ligand-donating ability of six bis-imine ligands. The electron-withdrawing character of bis-imine ligands has been linked to C-H activation in *N,N′*-bis-(pentafluorophenyl)-2,3-dimethyl-1,4-diaza-1,3-butadiene, and by replacing a fluorine with a nitrogen in *N,N′*-bis-(2,3,5,6-tetrafluoripyridine)-2,3-dimethyl-1,4-diaza-1,3-butadiene, the electronic density was localized on the pyridines leaving an electron poor imine region.

Table of Contents

Glossary

2-HC_2py……....2-ethynyl pyridine

Cp*……...pentamethyl cyclopentadienyl anion

DCM…….....dichloromethane

DMSO……..dimethyl sulfoxide

Et_2O…….....diethyl ether

^{F}DAB……...*N,N′* bis (pentafluorophenyl)-2,3-dimethyl-1,4-diaza-1,3-butadiene

LiHMDS…… lithium bis(trimethylsilyl)amide

^{n}BuLi……. n-butyl lithium

NEt_3……...……..triethylamine

$NH(iPr)_2$…….....diisopropylamine

NO_3…….....nitrate

OAc…….acetate

OTf…….....triflate

p-cym……...……*para*-cymene

PMe_3…….....trimethyl phosphine

PhC_2H……..ethynyl benzene

TFA…….....trifluoroacetate

THF…….....tetrahydrofuran

Chapter 1: Importance of Homogeneous Catalysis and Ligand Design

1. Fossil Fuel Conservation

Fossil fuels are non-renewable resources that contain a complex mixture of hydrocarbons that include the seven key building blocks in the chemical industry: benzene, toluene, xylene, ethylene, propylene, C_4 olefins, and synthesis gas.[1] Most economies depend on these fuels and have systems in place for extracting and transporting them. In 2006, a petroleum executive estimated that "there was enough coal in Earth's crust to last 164 years, enough natural gas to last 70 years, and only enough oil reserves for 40 years."[2] Further, the burning of these fuels is damaging to the environment. Around 35 billion tonnes of carbon dioxide are produced per year through this burning.[3] Energy efficient technologies are being studied extensively to conserve fuel to broaden the current reserve's lifetime and to slow the rate of atmospheric warming and ocean acidification. An example applicable to this thesis is the production of styrene, which is produced in over 18.5 million tons annually for packaging materials, insulation, medical devices, and other materials.[4] The current synthesis of styrene yields many disadvantages, and recent studies have shown a novel, efficient pathway for producing styrene to which we propose to contribute.

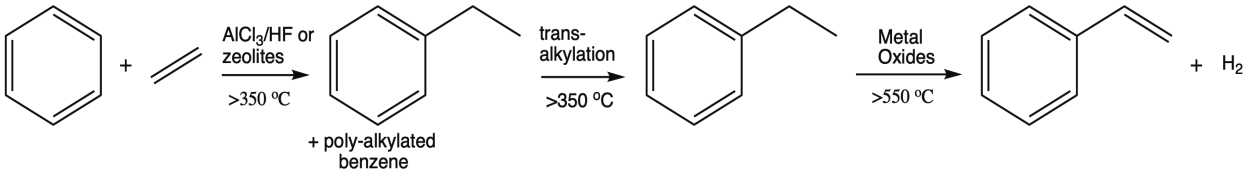

Scheme 1 Industrial styrene synthesis

In industry, styrene synthesis follows a multistep process: acid-catalyzed arene alkylation to first make ethylbenzene, trans-alkylation to optimize yield, then energy intensive dehydrogenation of ethylbenzene (Scheme 1).[5] The acid catalyst can be either a Friedel-Crafts reaction involving $AlCl_3$/HF or a zeolite catalyst; yet, both occur through the same electrophilic aromatic substitution mechanism involving the activation of ethylene.[6] In the Friedel-Crafts

catalysis, the reaction is exposed to harsh acids, and polyalkylation occurs to give a mixture of mono and *ortho*/*para* di-substituted ethylbenzenes. The low selectivity generates stoichiometric waste which makes the process highly inefficient for the broad goal of conserving fossil fuels. While zeolite catalysis is more sustainable than Friedel-Crafts, this process still requires high temperatures (350 °C – 450 °C) and has low selectivity.[5] Trans-alkylation occurs by moving the alkyl groups along the aromatic to achieve the desired ethylbenzene. Then, the reaction follows dehydrogenation which is an energy-intensive process to oxidize the C-H bonds from the ethyl group to make an equivalent dihydrogen and double bond between the carbons on the ethyl group. This is an endothermic process as well as kinetically inert requiring metal oxides as a catalyst and high temperatures.

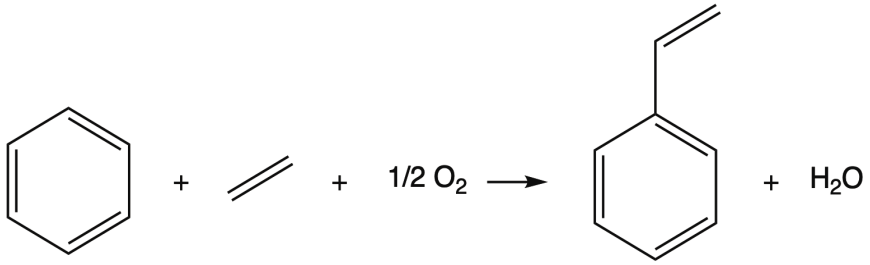

Scheme 2 Styrene production through C-H activation

An alternative pathway to produce styrene is by activating the C-H bond in benzene instead of activating the C-C bond in ethylene in the presence of an oxidant to remove a net equivalent of dihydrogen. The overall reaction is thermodynamically favorable, -67.9 kcal/mol (Scheme 2).[6] This research proposes to develop a new class of a metallohinged *trans*-bidentate ligand to study C-H activation of benzene with potential application as a catalyst for styrene production from benzene and ethylene.

2. C-H Activation

The selective functionalization of inert hydrocarbon C-H bonds is of interest because of its potential for improved routes of high-value fine chemicals, lower cost, and less chemical waste.[7] A C-H bond of an sp^3- and sp^2-hybridized hydrocarbons is not a traditionally reactive bond (pKa > 45-60 and BDE = 93 kcal/mol), and there is difficulty in selectivity because of the large presence in organic molecules.[8] Cleaving a C-H bond using a transition metal catalyst can directly form a new carbon-carbon or carbon-heteroatom bond (Scheme 3).

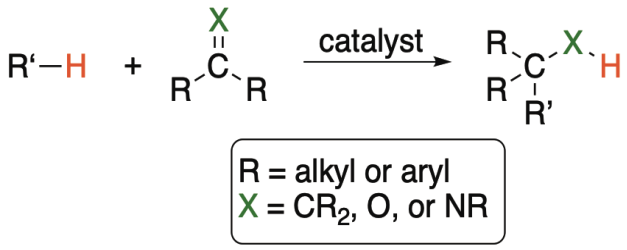

Scheme 3 C-H activation

Murai *et al.* reported a carbonyl(dihydrido)tris(triphenylphosphine)ruthenium(II) catalyst used for the direct addition of a C-H bond in an aromatic ketone to an alkene.[9] Further, reports of carboxylate-assisted C-H activation with an electron-deficient metal center have proven successful for breaking the unreactive C-H bond.[10] The carboxylate bases have a chelating ability which means they will remain bound to the metal as they facilitate deprotonation. In a theoretical study, the activation of benzene by $[M(\eta^2\text{-}O_2CH)_2]$ where M = Pd(II) or Pt(II) can easily achieve C-H activation because the formate ligands assist the activation through the formation of strong O-H bonds.[11]

Late transition metals such as Pd(II), Ir(III), Rh(III), Co(III), and Ru(II) have all been studied for C-H activation.[10] Acetate-assisted C-H activation with Pd(II) is shown in Figure 1. In this transition state, the R-H where R = alkyl or aryl and Pd-O of acetate is breaking simultaneously

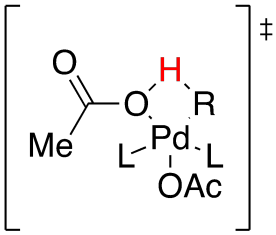

Figure 1 Transition state for Pd(II) acetate-assisted C-H activation

as the new Pd-R and O-H acetic acid bonds are forming. This transition in turn affects the bite angle of L-Pd-L to increase closer to an 180° conformation.[10] The displacement of the acetate ligand promotes access to the vacant sites of the metal center. Further, $Pd(OAc)_2$ is known to be an efficient catalyst for C-H activation.[12] Other metals such as rhodium and iridium have been modeled for the cyclometalation of *N*-alkylimines and 2-phenylpyridine at $[MCl_2Cp^*]_2$ where M = Rh(III) or Ir(III).[13] Co(III) C-H activation has also been studied because of the greater accessibility of {CoCp*} catalysts compared to {RhCp*} catalysts from the higher spin states for Co(II) and Co(III) oxidation states.[14] Even though the reaction was endergonic, the {CoCp*} species could form pyrroloindolones through the coupling of alkynes with *N*-dimethylcarbamoyl-indole.[14] Additionally, a computational DFT study showed that 2-phenylpyridine with $[RuCl_2(p\text{-cymene})]_2$ in presence of acetic acid and triethylamine could promote C-H activation as well.[15] Based on these examples of C-H activation, further analysis in electrophilic metals with electron-withdrawing groups will be studied for potential catalysts in the promotion of a C-H bond.

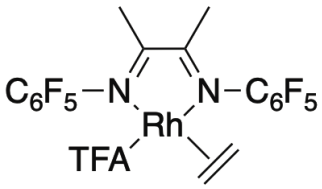

Figure 2 (^{F}DAB)Rh(TFA)(η^2-C_2H_4)

In the application of styrene production, it was found that a Rh(I) square planar complex with a neutral *cis*-bidentate imine ligand acted as a catalyst for rapid H/D exchange between benzene

and trifluoroacetic acid (TFA) (Figure 2).[16] The reaction follows a single step oxidative hydroarylation process in which C-H activation occurs on benzene.[6] DFT calculations show that the most active catalyst precursors contain electron-withdrawing substituents on the diimine ligands.[16] From this success, we explore an electron-deficient *trans*-bidentate ligand on a square planar Pd(II) and the computational design of new electron-deficient diimine ligands. While a *trans*-bidentate ligand can be used in catalysis, to our knowledge, this type of ligand has never been used in C-H activation, and diimine *N,N'*-bis-(2,3,5,6-tetrafluoripyridine)-2,3-dimethyl-1,4-diaza-1,3-butadiene is unknown.

3. Ligand Design

The identity of the ligand bound to the metal center is important to direct activity. Ligands can change the electronic properties and influence the steric environment of the metal coordination.[17] For instance, changing the ligand on a Ru(II) complex from PMe_3 to NHC (N-Heterocyclic Carbene) showed a much lower activation energy for alkene metathesis using the NHC.[18] Another type of ligand design is through chelation. Chelating ligands are commonly found in catalysts to increase stability and provide a higher degree of control over the coordination environment.[17] For example, *N,N-cis*-chelating Pd(II) complexes with bipyridines (bipy) are well known for C-H activation.[19] A bidentate ligand such as bipy is *cis* chelating where *cis* refers to the N-M-N bond angle at 90°. This leads to a natural question of whether a

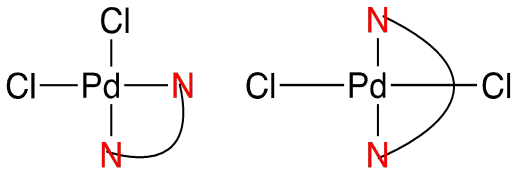

Figure 3 Cis vs trans ligand geometries

bidentate ligand with a 180° chelate as shown in Figure 3 would show similar or completely new reactivity to its *cis* counterpart.

Even though most bidentate ligands prefer a *cis* coordination, *trans*-bidentate ligands do exist.[20] *Trans*-bidentate ligands require donating groups at large distances which leads to potential issues in excessive flexibility and multiple coordination modes.[21] However, these rare *trans* ligands are useful in aiding complexes to achieve catalytic cycles. For instance, *trans*-spanning diphosphine ligands on a Pd(II) complex are effective precursors for Heck and Suzuki C-C coupling reactions.[20]

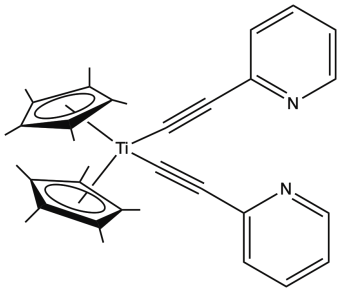

Figure 4 $Cp^*_2Ti(C_2$2-py)$_2$

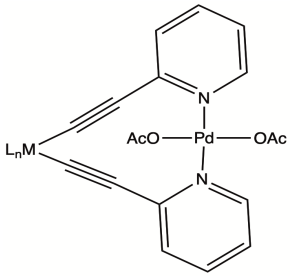

Figure 5 Trans-spanning ligand with $Pd(OAc)_2$

A method to force a *trans*-bidentate configuration is by first inserting two *cis*-alkynyl ligands to a complex. These ligands create a "hinge" which allow space for a new metal center to enter. An early example made by Bosch *et al.* of 1,2-bis(2-pyridyl-ethynyl)-benzene gave a rigid structure from the organic center with spacing between the pyridyl nitrogens measuring 3.86 Å through Spartan Plus computations.[21-23] Replacing benzene with a metal center such as Ti(IV) also coordinated the *cis*-ligands (Figure 4). The metalloligand $Cp^*_2Ti(C_2$-2-py$)_2$ could insert $Pd(Cl)_2$ but this complex has not been used before for C-H activation.[24] The metallohinge can be extended to other metals to form *cis*-alkynyl groups, and $Pd(OAc)_2$ can be inserted in between since it is useful in C-H activation (Figure 5). Since Pd(II) prefers a square planar

geometry, the pyridines are 180° apart from another when coordinated onto the metal center which creates a *trans*-bidentate ligand.

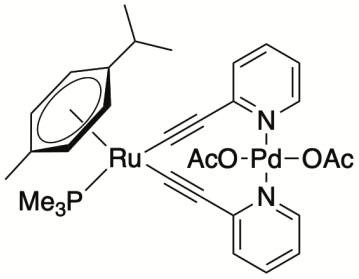

Figure 6 [(p-cym)Ru(PMe$_3$)(C$_2$-2-py)$_2$Pd(OAc)$_2$]

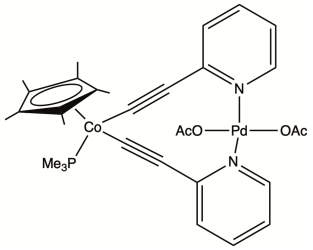

*Figure 7 [Cp*Co(C$_2$-2-py)$_2$Pd(OAc)$_2$]*

This research hypothesizes that other metals can be used to design a metallohinge, and we plan to utilize the low-spin d^6 metals Ru(II) or Co(III) in an octahedral field for C-H activation as these diamagnetic complexes are easily characterizable by NMR spectroscopy. The main catalyst of interest of [(*p*-cym)Ru(PMe$_3$)(C$_2$-2-py)$_2$Pd(OAc)$_2$] where (*p*-cym = *para*-cymene and C$_2$-2-py = 2-ethynyl pyridine) was studied for C-H activation on benzene (Figure 6). This is a square planar Pd(II) complex with an electron-deficient *trans*-bidentate ligand which can be compared to the known square planar Rh(I) complex with an electron-deficient *cis*-bidentate ligand.[6] Each part of [(*p*-cym)Ru(PMe$_3$)(C$_2$-2-py)$_2$Pd(OAc)$_2$] was chosen for a specific goal. Pd(II) was chosen based on precedent for effective C-H activation catalysis and on precedent for coordination as a *trans*-spanning ligand.[12,25] *Para*-cymene can help direct activity to the Ru(II) metal and also leave space for Ru(II) to coordinate to three other compounds all 90° apart. The phosphine in PMe$_3$ is flexible so that the compound can be characterized by NMR once the pyridines are added.[26] And the *cis*-alkynyl ligands attached are likely air stable and give space for Pd(OAc)$_2$ to coordinate.[27] A Co(III) complex [Cp*Co(C$_2$-2-py)$_2$Pd(OAc)$_2$] where (Cp* = pentamethyl cyclopentadienyl anion) is also of interest to replace the precious metal Ru(II) (Figure 7). The proposed complexes of [(*p*-cym)Ru(PMe$_3$)(C$_2$-2-py)$_2$Pd(OAc)$_2$] and [Cp*Co(C$_2$-2-py)$_2$Pd(OAc)$_2$] are hypothesized to activate the C-H bond in benzene in order to produce styrene through an energy-efficient catalytic cycle.

Electron-poor ligands attached to Rh(I) metal centers were found to be effective catalytic precursors for C-H activation on benzene.[6] Designing a ligand with electron-withdrawing groups to coordinate to the metal assists the electrophilic substitution reaction of C-H activation. Six imine ligands with varying electronics will also be studied to see which imine will give the most electron-poor compound.

4. Proposed Catalytic Cycle

The current method for producing styrene is inefficient, and a more selective process needs to be utilized in order to preserve the finite supply of hydrocarbon reserves. Using C-H activation to produce styrene is an atom-economical alternative to bypass energy intensive procedures. It has already been shown that [(^{F}DAB)Rh(TFA)(η^2-C_2H_4)] where (^{F}DAB = *N,N′* bis (pentafluorophenyl)-2,3-dimethyl-1,4-diaza-1,3-butadiene; TFA = trifluoroacetate) can be used to activate the C-H bond in benzene through oxidative hydroarylation.[6] This electron deficient, *cis*-bidentate ligand on square planar Rh(I) can be compared to a novel electron deficient, *trans*-bidentate ligand on square planar Pd(II). We believe a *trans*-bidentate ligand has the potential to follow the same oxidative hydroarylation pathway as the Rh(I) based on the interesting reactivities *trans* catalysts possess (Figure 8).

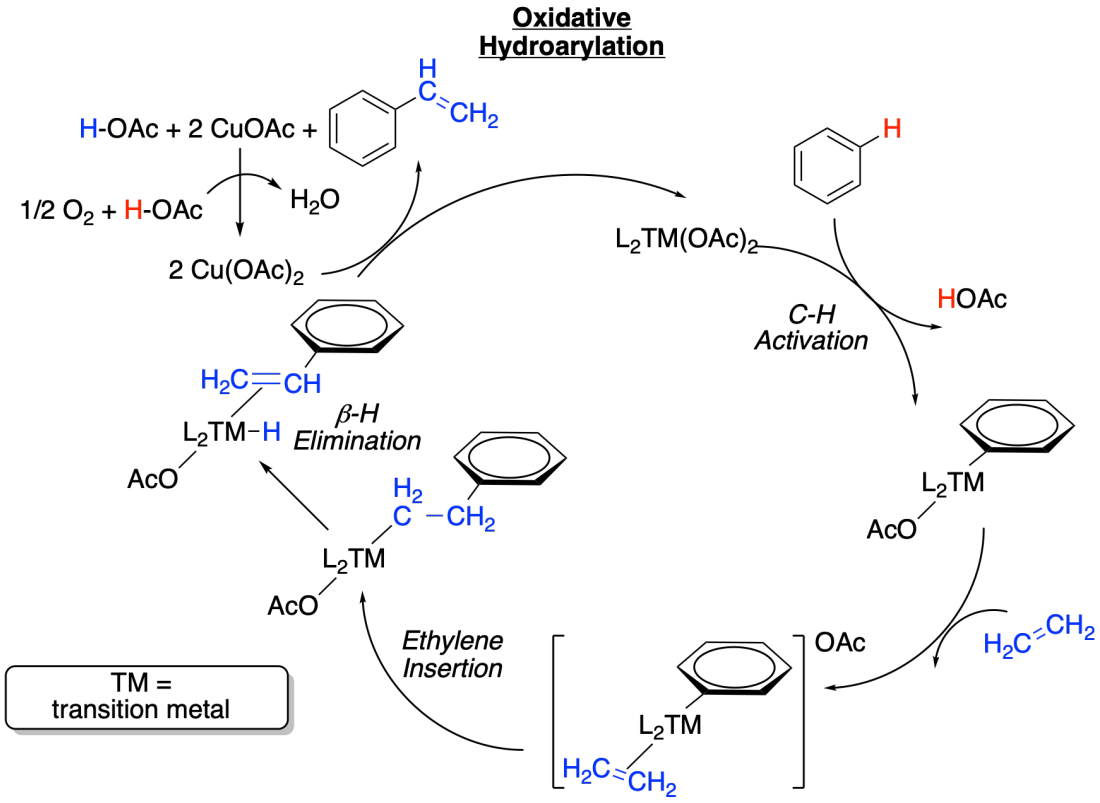

Figure 8 Proposed catalytic cycle of oxidative hydroarylation

The oxidative hydroarylation process can be broken down into three main steps: C-H activation on benzene, ethylene coordination and insertion, and beta-hydride elimination. The C-H bond on benzene is activated by acetate accepting the hydrogen off benzene to make acetic acid and the rest of the transition metal catalyst remains attached to benzene. Ethylene then coordinates and undergoes a 1,2-insertion into the Pd-C bond to produce Pd-CH_2CH_2Ph. The Pd-H hydrogen is removed and Pd(II) is reduced to Pd(0) through beta-hydride elimination. The Cu(II) acetate oxidizes the Pd(0) back to Pd(II) to regenerate the original catalyst and is reduced to Cu(I) acetate. In the presence of oxygen, Cu(I) acetate is re-oxidized to Cu(II) acetate and oxygen is reduced to water. Thus, the two hydrogens removed end up forming a water molecule to balance the overall reaction.

The cycle is similar to C-C coupling reactions such as the Heck reaction, except the C-H bond is activated instead of C-X and after ethylene insertion, the substrate undergoes beta-hydride

elimination to make the C-C double bond. This alternate pathway to activate benzene through C-H activation using [(^{F}DAB)Rh(TFA)(η^2-C_2H_4)] produces styrene in a single step with 100% selectivity, turnover numbers (TON) > 800, and is a thermodynamically favorable process.[6] Past transition metals used for oxidative hydrophenylation with inactivated substrates usually suffer from low yield, low TON, and poor selectivity to produce styrene.[6] For example, $(acac)_2Rh(Cl)(H_2O)$ where (acac = acetylacetonate) with $Cu(OAc)_2$ gave a selectivity of 89 % but with TONs of 24 and yield of 36 % styrene.[28] The catalyst of $Rh(PMe_3)_2(CO)(Cl)$ using light gave a TON of 3, and low selectivity and yield to produce styrene as well.[29] Interestingly, both complexes utilize highly electron rich ligands such as acetylacetonate and trimethylphosphine. The syntheses examined in the next chapter follow the unique design of creating a *trans*-bidentate ligand from *cis*-alkynyl ligands to explore the potential effectiveness of catalysis by activating the C-H bond in benzene. The chapter following will explore electron-withdrawing imine ligands to see which ligand has the potential to give the most effective catalyst.

5. References

1. IHS Chemical Training: Understanding the petrochemical industry. https://chemweek.com/CW/Document/58961/IHS-Chemical-Training-Understanding-the-petrochemical-industry (accessed April 6, 2021).
2. Why Should We Conserve Fossil Fuels? https://sciencing.com/about-6297325-should-conserve-fossil-fuels-.html (accessed January 21, 2021).
3. Fossil Fuel. https://en.wikipedia.org/wiki/Fossil_fuel (accessed February 23, 2021)
4. Styrene / Polystyrene Uses and Benefits - You Know Styrene. https://youknowstyrene.org/the-styrene-you-know/uses-and-benefits/ (accessed Oct 14, 2019).
5. Vaughan, B. A.; Webster-Gardiner, M. S.; Cundari, T. R.; Gunnoe, T. B. *Sci.* **2015**, *348*, 421-424.
6. Vaughan, B. A.; Khani, S. K.; Gary, J. B.; Kammert, J. D.; Webster-Gardiner, M. S.; McKeown, B. A.; Davis, R. J.; Cundari, T. R.; Gunnoe, T. B. *J. Am. Chem. Soc.* **2017,** *139*, 1485-1498.
7. Liebov N.S. et al. *Materials Science*, **2021**, *284*.
8. Thansandote, P.; Lautens, M. Chem. Eur. J. **2009**, *15*, 5874.
9. Murai, S.; Kakiuchi F.; Sekine, S.;Tanaka, Y.; Kamatani, A. *Nature* **1993**, *366*, 529.
10. Davies, D. L.; MacGregor, S. A.; McMullen C. L. *Chem. Rev.* 2017, *117*, 8649-8709.
11. Biswas, B.; Sugimoto, M.; Sakaki, S. *Organometallics*, **2000**, *19*, 3895.
12. Choy, P. Y.; Lau C. P.; Kwong, F.Y. *J. Org. Chem.* **2011**, *76*, 80-84.
13. Tang, H.; Zhou, B.; Huang, X.-R.; Wang, C.; Yao, J.; Chen, H. *ACS Catal.* **2014**, *4*, 649−656.
14. Carr, K. J. T.; Macgregor, S. A.; McMullin, C. L.Wiley-VCH Verlag GmbH & Co. KGaA: New York, **2016**.
15. Ikemoto, H.; Yoshino, T.; Sakata, K.; Matsunaga, S.; Kanai, M. *J. Am. Chem. Soc.* **2014,** *136,* 5424−5431.
16. Gray, A.; Tsybizova, A.; Roithova, J. *Chem. Sci.* **2015**, *6*, 5544−5553.
17. Webster-Gardiner, M. S.; Piszel, P. E.; Fu, R.; McKeown, B. A.; Nielsen, R. J.; Goddard, W. A., III; Gunnoe, T. B. **2017**, *426*, 381-388.
18. Lundgren, R. J.; Stradiotto, M. Wiley-Blackwell: **2016**; 1-14.
19. Durand, D. J.; Fey, N. **2019,** *119*, 6561-6594.
20. Wang, N; McCormick, T. M.; Ko, S.; Wang, S. *Euro. J. Inorg. Chem.* **2012**, 4463-4469.
21. Comanescu, C. C.; Iluc, V. M. *Inorg. Chem.* **2014,** *53*, 8517-8528.
22. Kaganovsky, L.; Cho, K.-B.; Gelman, D. *Organometallics* **2008,** *27*, 5139-5145.
23. Pereira, F. A.; Fallows, T.; Frank, M.; Chen, A.; Clever, G. H. *Z. Anorg. Allg. Chem.* **2013**, 1598-1605.
24. Bosch, E.; Barnes, C. L. *Inorg. Chem.* **2001,** *40*, 3097-3100.
25. Vieira N.C.; Pienkos J.A.; McMillen C.D.; Myers A.R.; Clay A.P.; Wagenknecht P.S. *Dalton Trans.,* **2017**, 46, 15195.
26. Lee, J. P.; Hankins, M. J.; Riner, A. D.; Albu, T. V., *J. Coord. Chem.* **2016,** *69*, 20-38.
27. Menendez, C.; Morales, D.; Perez, K.; Riera, V. *Organometallics*. **2001**, *20*, 2775-2781.
28. D. Taube, R. Periana, T. Matsumoto (U.S. Patent 6127590A, **2000**).

29. Sasaki, K.; Sakakura, T; Tokunaga, Y.; Wada, K.; Tanaka, M. *Chem. Lett*. **1988**, *17*, 685–688.

Chapter 2: Synthesis and Characterization of Low Spin d^6 Complexes with a *Cis*-alkynyl Metallohinge for *Trans*-spanning Ligands

1. Introduction

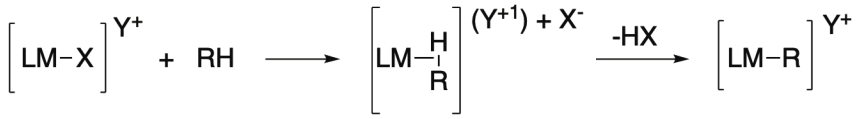

Scheme 1 Electrophilic Substitution Reaction

Electrophilic metals can act as catalysts for alkane and arene C-H functionalization through an electrophilic substitution reaction (Scheme 1). Examples of electrophilic metals used for C-H activation have been Hg(II), Pd(II), and Pt(II).[1] Generally, it is more difficult to achieve selective functionalization in alkanes than arenes since they are relatively unreactive.[1] This research studies an electrophilic aromatic substitution reaction on benzene. A recent report of a Rh(I) complex [(^{F}DAB)Rh(TFA)(η^2-C_2H_4)] where (^{F}DAB = *N,N′*-bis(pentafluorophenyl)-2,3-dimethyl-1,4-diaza-1,3-butadiene; TFA = trifluoroacetate) was used for catalytic H/D exchange on benzene.[1]

Regardless of emerging C-H activation reactions or ubiquitous cross coupling reactions, ligand identity plays a crucial role in reactivity.[2,3] Many ligands used in catalysis are chelating ligands. Specific chelating ligands that can "bite" into the metal center at two locations are called

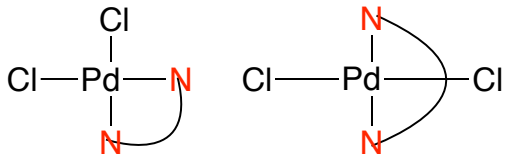

Figure 1 Cis vs trans geometries

bidentate ligands. These ligands can range from the *cis*-isomer of 90° to the *trans*-isomer of 180° (Figure 1). *Cis*-chelating nitrogen donor ligands are commonly known such as 2,2'-bipyridine (bpy) and 1,10-phenanthroline (phen) because of their high stability and diverse properties.[4] *Trans*-bidentate ligands are less studied because most bidentate ligands have a strong preference to *cis* coordination.[2] However, the known *trans*-bidentate ligands may exhibit

properties not observed in *cis* ligands. For instance, the larger bite angle in a *trans* diphosphane ligand allowed easier access of the substrate to the Pd(II) center in the C-H activation step.[3] The *trans*-chelating ligands in this research will be explored for their catalytic reactivities in C-H activation.

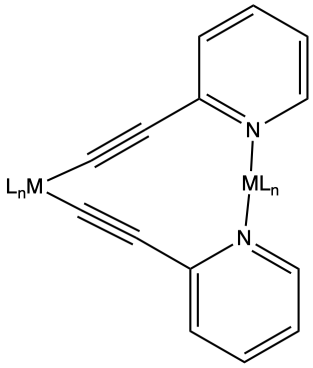

Figure 2 Metallohinged complex

A method of forming a *trans*-bidentate ligand is using a transition metal hinge (Figure 2). This metallohinge has *cis*-alkynyl ligands set in place in order for a new metal to coordinate to the nitrogen donors on the pyridine rings in a *trans* fashion. For example, the Ti(IV) *cis*-alkynyl complex $[Cp^*_2Ti(C_2\text{-}2\text{-}py)_2]$ where (Cp* = pentamethyl cyclopentadienyl anion, C_2-2-py = 2-ethynyl pyridine) was able to coordinate to a Pd(II) metal in a *trans*-spanning arrangement.[5]

As late transition metals are capable of C-H activation, this research studies d^6 organometallic fragments such as {(*p*-cym)Ru(II)} and {Cp*Co(III)} as metallohinges. The

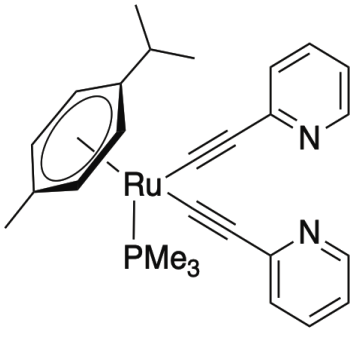

*Figure 3 [(p-cym)Ru(PMe_3)(C_2-2-py)$_2$] (**1**)*

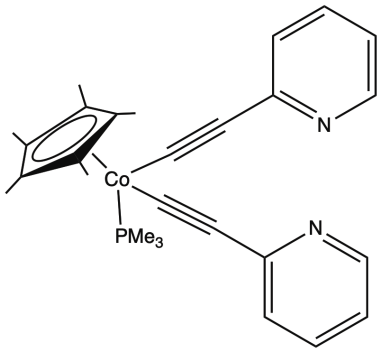

*Figure 4 [Cp^*Co(PMe_3)(C_2-2-py)$_2$] (**2**)*

main complex of interest is the octahedral [(*p*-cym)Ru(PMe_3)(C_2-2-py)$_2$] (**1**) (Figure 3). The electron rich *p*-cym coordinates to three sites of the Ru(II) metal center facially which makes the other three ligands all *cis* to each other. PMe_3 is a strong sigma-donor the Ru(II) metal center thus stabilizing the complex.[6,7] The phosphorus ligand is important for characterization (e.g. ^{31}P NMR), and the groups attached to phosphorus can be replaced to modulate the electron density at the metal center. The *cis*-alkynyl ligands will create the metallohinge to provide space for another metal complex to be inserted with the pyridine nitrogens forcing a *trans* coordination to the second metal. Additionally, this complex is likely air-stable and can be compared to the known complex of [(*p*-cymene)Ru(PMe_3)(C_2-Ph)$_2$] where (C_2-Ph = ethynylbenzene) and the same procedure can be followed for **1**.[8]

Another aspect of this research involves replacing the precious metal Ru(II) in **1** with an Earth-abundant metal like Co(III) for [Cp^*Co(PMe_3)(C_2-2-py)$_2$] (**2**) (Figure 4). The Co octahedral complex has a similar ionic radii to the known complex of [Cp^*_2Ti(C_2-2-py)$_2$] (Co(III), 0.55 Å, vs Ti(IV), 0.60 Å).[9,10] Additionally, the electron-deficient Co(III) has a reduced π-basicity and is not likely to π-back-bond with alkynyl ligands, which increases the chances for a Pd(II) center to be coordinated in a *trans* fashion because of its flexibility.[11] If these *trans*-bidentate metals can be synthesized with a Pd(II) complex, the efficiency of catalytic activity for C-H activation can be investigated.

2. Experimental Section

2.1 Materials

All reactions and procedures were performed under anaerobic conditions in a nitrogen-filled glovebox or using standard Schlenk techniques. Glovebox purity was maintained over a

catalyst bed and monitored by an oxygen analyzer (O_2 (g) < 2 ppm for all reactions). Dichloromethane was purified by distillation from calcium hydride. Hexanes were purified by distillation from sodium. Tetrahydrofuran was purified by distillation from sodium/benzophenone. C_6D_6 and $CDCl_3$ were degassed via three freeze–pump–thaw cycles and stored over 4 Å sieves. The ^nBuLi, PhC_2H, Et_2O, AgOTf, $AgNO_3$, NEt_3, KPF_6, CuI, $NH(iPr)_2$, $Pd(OAc)_2$, 2-HC_2py, and LiHMDS were purchased from either Aldrich Chemical Company or Acros Organics and used as received. The metal reagents [(*p*-cym)Ru(PMe_3)$(Cl)_2$] and [Cp*Co(PMe_3)$(I)_2$] were prepared as previously reported.[7] All other reagents were used as purchased from commercial sources.

2.2 Measurements

^1H and ^{13}C NMR spectra were obtained on a JEOL ECX 400 MHz spectrometer (operating frequency for ^{13}C NMR was 100 MHz) and referenced against tetramethylsilane using residual proton signals (^1H NMR) or the ^{13}C resonances of the deuterated solvent (^{13}C NMR). ^{31}P spectra were obtained on a JEOL ECX 400 MHz (operating frequency = 162 MHz) spectrometer and referenced against external 85% H_3PO_4 (0 ppm).

2.3 Syntheses

2.3.1 Preparation of [(*p*-cym)Ru(PMe_3)$(Cl)_2$]

[(*p*-cym)Ru$(Cl)_2]_2$ (0.1009 g, 0.16 mmol) and THF (15 mL) was added to an oven-dried 50 mL Schlenk under N_2 to produce a cloudy heterogeneous orange solution. PMe_3 (0.36 mL, 0.36 mmol) was added via syringe to make a homogenous red/orange solution. After 1 h, THF was reduced to a minimal amount by rotary evaporator, then hexanes were added to the product and filtered out by vacuum filtration. The orange solid was isolated (0.1186 g, 94.2% yield). ^1H

NMR (400 MHz, Chloroform-*d*) δ 5.39 (s, 4H), 2.82 (sep, 1H), 2.04 (s, 3H), 1.56 (d, 9H), 1.18 (d, 6H). ^{31}P NMR (162 MHz, Chloroform-*d*) δ 4.74.

2.3.2 Preparation of [Cp*Co(PMe_3)(I_2)]

[Cp*Co(CO)(I_2)] (0.2316 g, 0.48 mmol) and DCM (15 mL) was added to an oven-dried 50 mL Schlenk under N_2 to produce a dark black solution. PMe_3 (0.54 mL, 0.54 mmol) was added to the dark solution and gas evolution (presumably CO) was observed. After 6 h, the solvent was reduced to a minimal amount on the rotary evaporator. Diethyl ether was added and the product was collected by vacuum filtration. A dark blue solid was obtained (0.1360 g, 56% yield). ^{1}H NMR (400 MHz, Chloroform-*d*) δ 1.94 (d, 15H), 1.88 (d, 9H).

2.3.3 Preparation of [(*p*-cym)Ru(PMe_3)(C_2-2-py)$_2$] (**1**) using LiHMDS

An oven-dried 100 mL Schlenk flask was brought inside the purged glovebox. LiHMDS (0.193 g, 1.15 mmol), a 0.9901 M of 2-HC_2py in THF (1.14 mL, 1.15 mmol), and THF (5 mL) was added to the flask to make a heterogeneous brown solution with a white precipitate. After 30 min of stirring, the solution became a heterogeneous burgundy color and [(*p*-cym)Ru(PMe_3)(Cl_2)] (0.200 g, 0.522 mmol) was added to the Schlenk flask to give a dark brown heterogeneous solution. After 6 h of stirring, the solution was homogeneous dark brown, and the THF was removed *in vacuo* inside the glovebox leaving a dark brown solid. Benzene (2 mL) was added to the Schlenk flask to dissolve leftover LiHMDS. After 16 h, diethyl ether (1 mL) was added to the Schlenk flask and this solution was poured into a frit and filter flask for vacuum filtration. The Schlenk flask was rinsed with more benzene (5 x 2 mL) and poured into the frit. A brown/ coffee powder solid was isolated on the frit (0.1256 g, 46.5% yield). ^{1}H NMR (400 MHz, Chloroform-*d*) δ 8.40 (d, J = 4.74 Hz, 2H), 7.41 (td, J = 7.70 Hz, J = 1.79 Hz, 2H), 7.23 (d, J = 8.00 Hz, 2H), 6.90 (td, J = 5.80 Hz, J = 1.42 Hz, 2H), 5.63 (d, 2H), 5.58 (d, 2H) 2.86

(sep, 1H), 1.71 (d, J = 10.26 Hz, 9H), 1.30 (d, J = 6.84 Hz, 6H). ^{31}P NMR (162 MHz, Chloroform-*d*) δ 15.24.

3. Results and Discussion

The synthesis of [(*p*-cym)Ru(PMe_3)(C_2-2-py)$_2$] (**1**) could potentially start from the Ru(II) dimer of [(*p*-cym)Ru(Cl)$_2$]$_2$ or [(*p*-cym)Ru(PMe_3)(Cl)$_2$]. The former would be a single-pot two-step process. Neither the dimer nor the trimethylphosphine intermediate showed a difference in results for making **1**. The intermediate [(*p*-cym)Ru(PMe_3)(Cl)$_2$] was used as starting material for the future Ru(II) reactions because of its ease of preparation, and knowing exactly what I was working with. The ^{31}P NMR signal for [(*p*-cym)Ru(PMe_3)(Cl)$_2$] was 5 ppm.

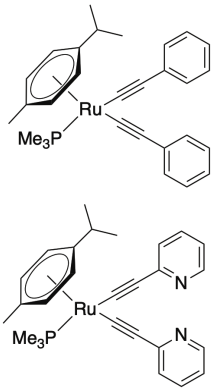

*Figure 5 Comparing [(p-cym)Ru(PMe_3)(C_2-Ph)$_2$] to **1***

As the main goal is to create a *trans*-bidentate ligand, first *cis*-alkynyl ligands need to be attached to the complex to create the metallohinge. The initial experimental set-up follows synthesizing the known complex of [(*p*-cym)Ru(PMe_3)(C_2-Ph)$_2$] where (C_2-Ph = ethynyl benzene) which contains the ideal *cis* angle from the alkynes on Ru(II) metal.[8] This was a good starting point because if this complex could be repeated based on the literature set-up, then [(*p*-cym)Ru(PMe_3)(C_2-2-py)$_2$] (**1**) where (C_2-2-py = 2-ethynyl pyridine) can be prepared analogously

because of their similar structure (Figure 5). However, the known complex was challenging to make with ^{n}BuLi as the base and the experimental set-up can be found in Appendix 1 (A.1). 2.2, 4.0, and 10.0 molar equivalents of ^{n}BuLi and 2-HC_2Ph were attempted to make [(*p*-cym)Ru(PMe_3)(C_2-Ph)$_2$] with either no reaction or partial conversion (i.e., [(*p*-cym)Ru(PMe_3)(C_2-Ph)(Cl)]).

A new leaving group, triflate from silver, was introduced to make [(*p*-cym)Ru(PMe_3)(OTf)$_2$] where (OTf = triflate) in an attempt to detach from the complex easier than the chlorides (A.2). Even though triflate is a better leaving group since the sulfonate ion can stabilize the negative charge by resonance, no reaction occurred when trying to attach 2-HC_2Ph with ^{n}BuLi.

A known complex AgC_2Ph, was synthesized using a reported procedure.[12] AgC_2Ph is air stable and a solid and this was to be mixed with [(*p*-cym)Ru(PMe_3)(Cl)$_2$] to make [(*p*-cym)Ru(PMe_3)(C_2-Ph)$_2$] (A.3). This reaction was attempted in efforts to have a simpler reaction set-up where it was less prone to error since it did not need to be under N_2 and the reactant was measured in solid form. However, based on ^{31}P NMR no reaction was observed.

After these previous attempts, the research moved to synthesize **1**. To avoid using a microliter syringe, an approximate 1 M (0.9901 M) 2-HC_2py in THF standard was made. With this new technique, **1** was synthesized using two molar equivalents of ^{n}BuLi and 2-HC_2py with a stir time of 4 or 24 h and gave around a 30% yield (A.4). Although, using ^{n}BuLi remained challenging because it often yielded inconsistent results for the same experimental set-up. 2.0, 2.2, 2.5, 4.0, and 10.0 molar equivalents were all tried for 2-HC_2py and ^{n}BuLi, but consistent results were not obtained.

New reactants such as KPF_6 was used to make **1** but the desired product was not made (A.5). This reaction was attempted so KPF_6 could remove the chlorides from [(*p*-cym)Ru(PMe_3)($Cl)_2$] and NEt_3 deprotonates the base.[13] Additionally, the reactant CuI was used as a catalyst to make **1** because *cis*-alkynl ligands were able to be attached to (tbpy)$PtCl_2$ which is a complex that has similar electronic character to the desired **1** (A.6).[14] The CuI coordinates to the alkyne triple bond and increases the acidity of the C-H bond while the amine deprotonates the C-H bond. But this gave missing peaks for the Ru(II) complex which suggests Ru(II) oxidized to Ru(III).

Finally, a new base, lithium bis(trimethylsilyl)amide (LiHMDS) was tried to help with stoichiometric errors and this is stated in the experimental section. The LiHMDS was the best base to deprotonate 2-HC_2py for the reaction to make the desired complex of **1** because it could be transferred as a solid at room temperature. Originally, the base added to the reaction was in liquid form, but now that the base can be added as a solid, it is easier to transfer. The reaction gave consistent results to form complex **1** based on NMR characterization with yields consistently around 40%. However, even though **1** is the main complex characterized in the NMR, starting material and the mono-substituted version are present as well in a lesser amount.

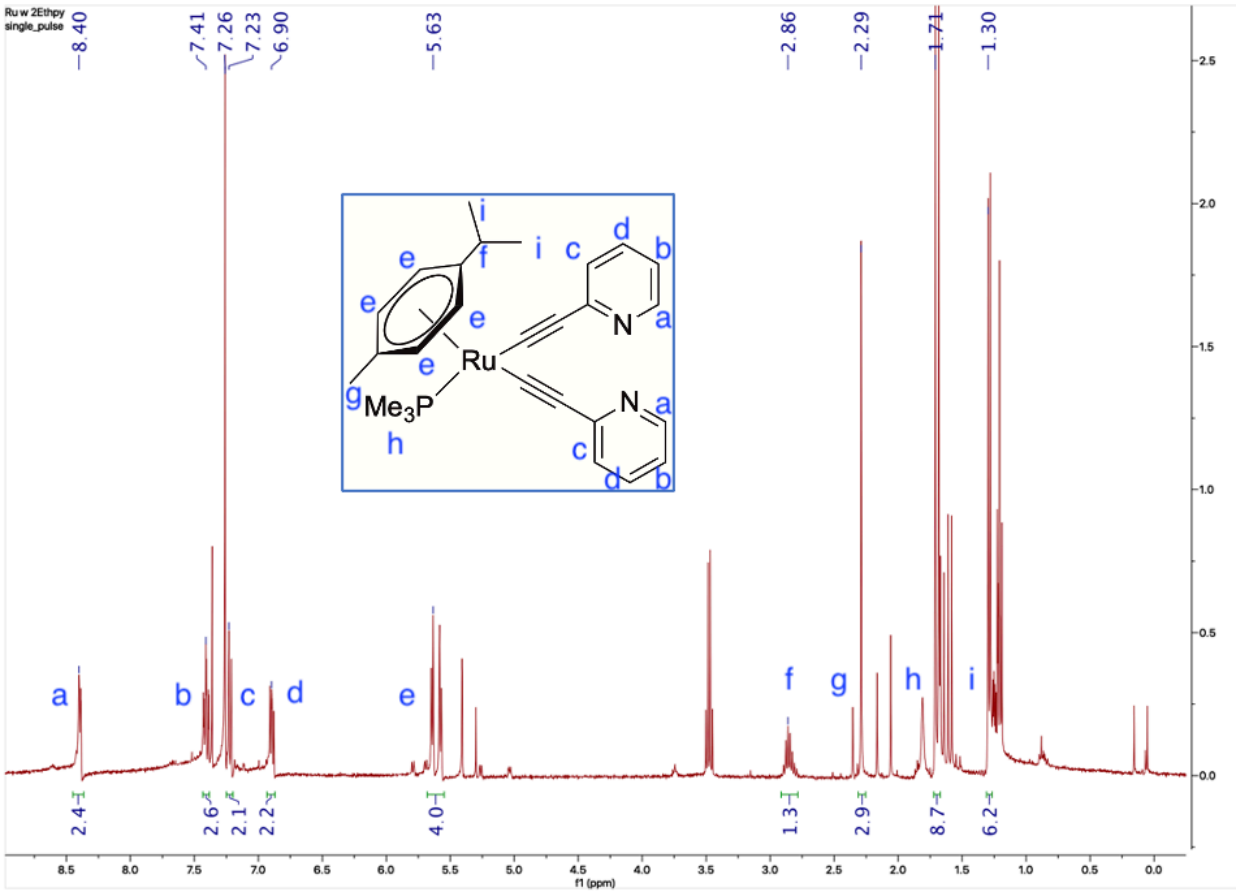

*Figure 6 Full [1]H NMR of **1***

The full [1]H NMR of **1** is shown (Figure 6). The total integration accounts for the 31 hydrogens on the complex. Leftover starting material and impurities such as acetone, benzene, tetrahydrofuran, hexanes, and the bis(trimethylsilyl)amide are also present.[15]

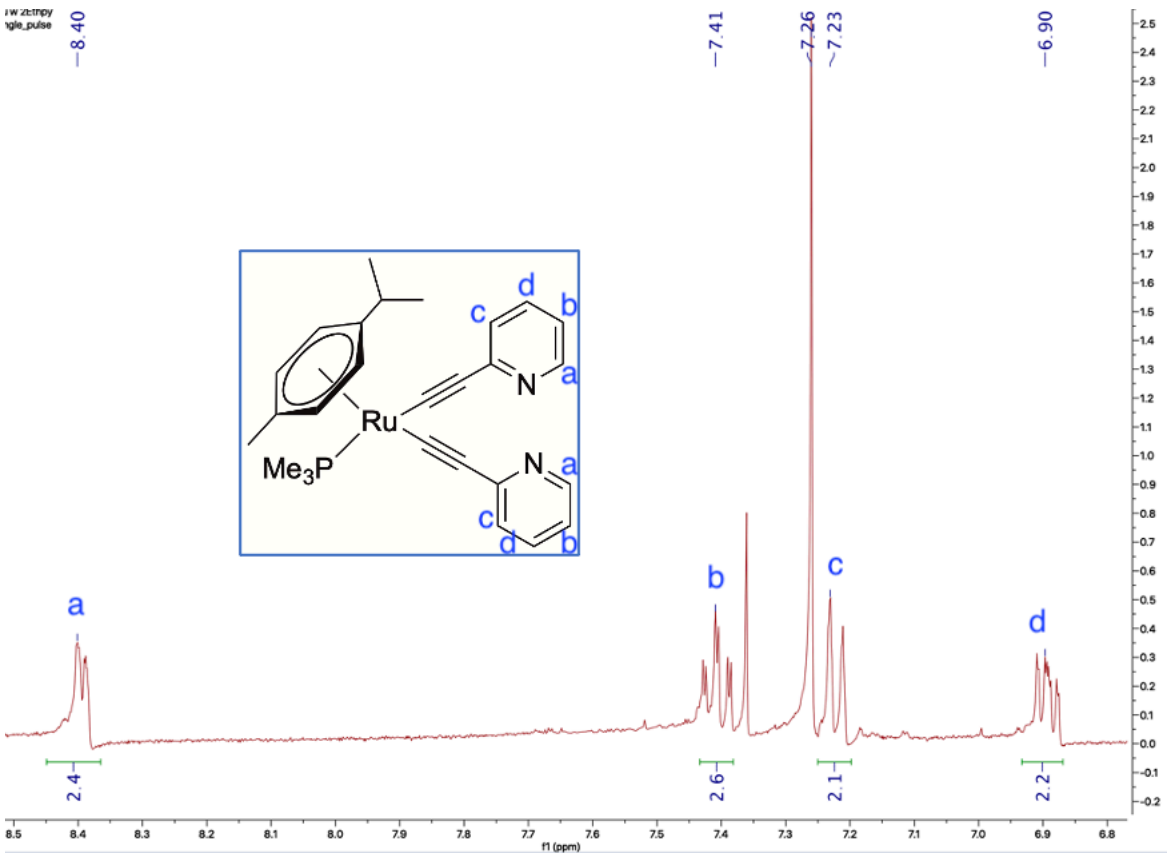

*Figure 7 Downfield ^{1}H NMR of **1***

The downfield region is shown (Figure 7). This section accounts for the eight total hydrogens on the pyridines as these are the least shielded. Each signal represents the same hydrogen position for both pyridines which is why they integrate for roughly two protons each. The hydrogen closest to the nitrogen is furthest downfield which moved from 8.55 ppm in 2-ethynyl-pyridine prior to deprotonation and coordination. There is a singlet around 7.36 from residual benzene which slightly interferes with the complex's signal at 7.41 which could indicate why the integration was slightly higher there.[15]

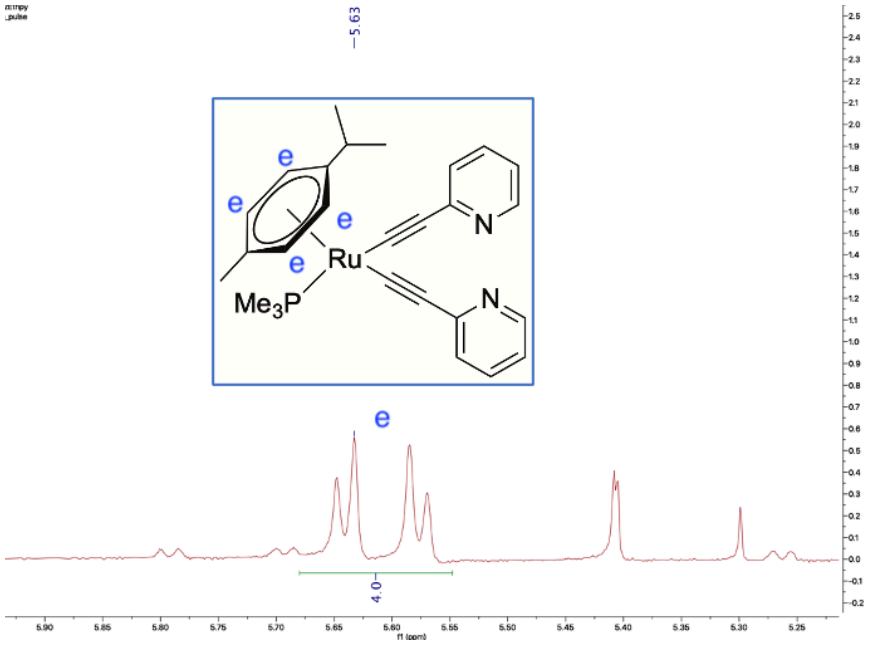

*Figure 8 Midfield ^{1}H NMR of **1***

The midfield region contains the four aromatic hydrogens on *p*-cymene as two doublets (Figure 8). From this close-up on the *p*-cymene, the complex has mirror symmetry bisecting the two alkynyl ligands. The small doublets around 5.80 ppm, 5.70 ppm, 5.28 ppm, and 5.14 ppm could be the mono-substituted version of this complex ([(*p*-cym)Ru(PMe_3)(C_2-Ph)(Cl)]). At 5.40 ppm, this is the starting material. And, 5.30 ppm is DCM impurity.[15]

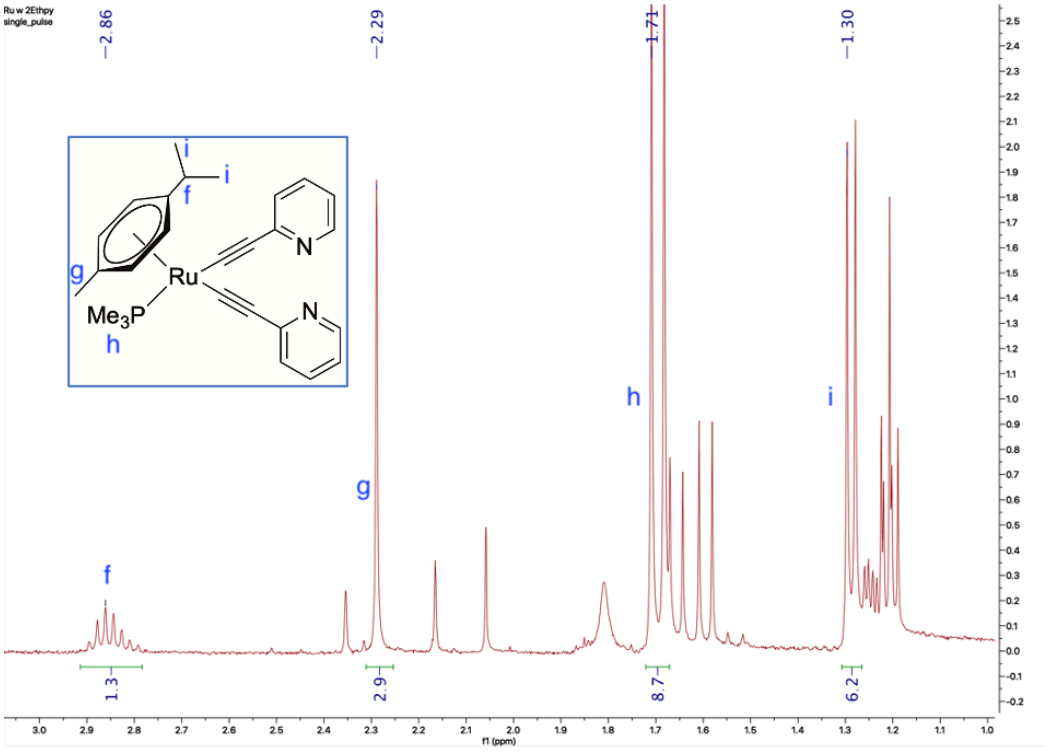

*Figure 9 Upfield ^{1}H NMR of **1***

The upfield region shows the most shielded signals from the isopropyl and methyl groups (Figure 9). The septet at 2.86 ppm is the isopropyl hydrogen. The singlet at 2.29 ppm represents the methyl group on *p*-cymene. The doublet at 1.71 ppm is the signal for the nine hydrogens on trimethylphosphine. Lastly, the most upfield doublet is the six hydrogens off the isopropyl group branches. There are many impurities in the upfield region from acetone (2.17 ppm), tetrahydrofuran (1.85 ppm), or leftover starting material.[15] Also the bis(trimethylsilyl)amide by-product at 0.00 ppm can be seen from Figure 6. The starting material peaks are the smaller signals more upfield than their corresponding peaks from **1**. Work is ongoing for a successful purification technique such as column chromatography.

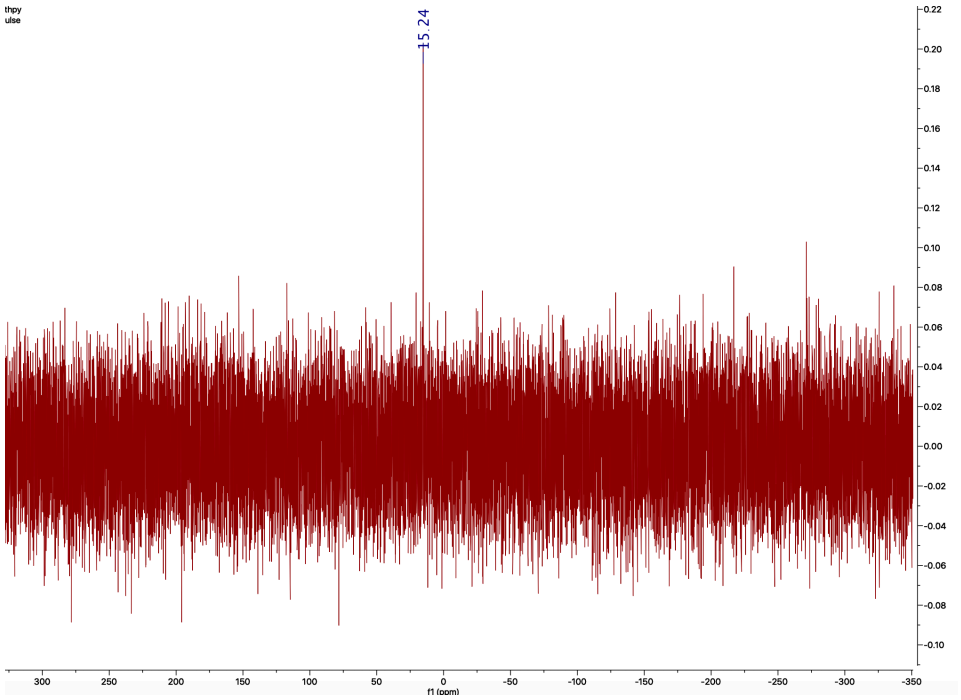

*Figure 10 ^{31}P NMR of **1***

The ^{31} P NMR is the best indication that compound **1** was made (Figure 10). The complex of [(*p*-cym)Ru(PMe_3)$(Cl)_2$] has a signal at 5 ppm which is consistent with literature.[8] We report a shift to 15 ppm for the complex [(*p*-cym)Ru(PMe_3)$(C_2Ph)_2$] and this shift is expected for **1** since the only difference is replacing the phenyl rings for pyridyl rings.[8] Since the trimethylphosphine shifted positions, this is an indication that **1** was made. There were several challenges to purify and/or crystallize **1**. Unfortunately, **1** was not completely soluble in most solvents (Table 1).

Table 1: Solubility Test of [(*p*-cym)Ru(PMe_3)(C_2-2-py)$_2$]	
Solvent	**Solubility**
Acetonitrile	Insoluble
Acetone	Insoluble
Tetrahydrofuran	Partially soluble
50/50 Acetonitrile/ Tetrahydrofuran	Soluble
Methanol	Soluble
Benzene	Partially soluble
Diethyl ether	Insoluble
Hexane	Insoluble
Toluene	Partially soluble
Dichloromethane	Soluble

The lack of solubility affected the crystallization attempts as well. A single-crystal X-ray structure is ongoing to finish characterization. Some crystals were able to be obtained, but none have been good enough to diffract. The most successful crystallization techniques were layering by dissolving the solid in dichloromethane and layering with hexanes, layering by dissolving the solid in tetrahydrofuran and layering with diethyl ether, and slow diffusion by dissolving the solid in benzene with diethyl ether diffusing into the crystallization tube. Moreover, there were initial troubles to remove the amine (Scheme 2).

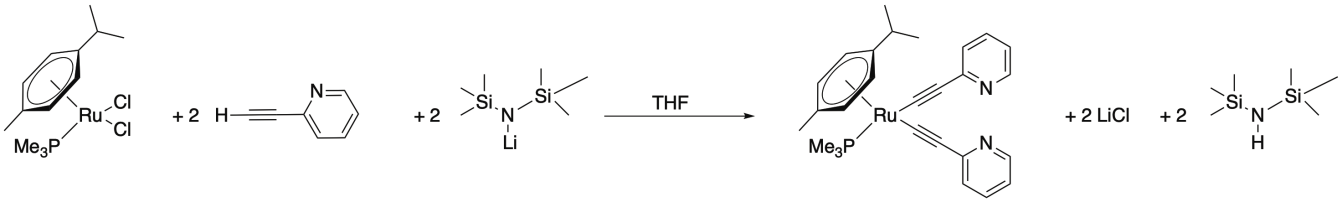

*Scheme 2 Synthesis of **1***

The signals around 0 ppm in Figure 6 of the full NMR show that the amine is still present in the isolated mixture. Rinsing the solution with benzene and diethyl ether would dissolve most of the ammine and keep the product. Before adding this step, the signals from the amine were double the size of the product peaks.

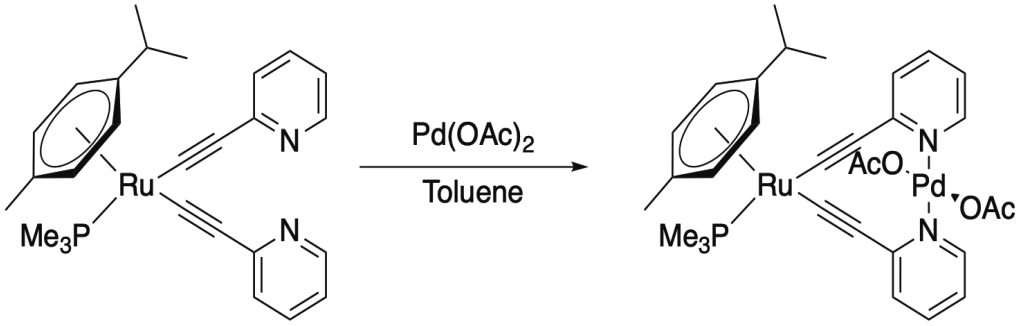

Scheme 3 [(p-cym)Ru(PMe$_3$)(C$_2$-2-py)$_2$Pd(OAc)$_2$]

The next step is inserting $Pd(OAc)_2$ between the nitrogens on each pyridine in **1** as a *trans*-bidentate ligand (Scheme 3). $Pd(OAc)_2$ was chosen because of its many uses in various catalytic reactions.[16] The insertion of $Pd(OAc)_2$ to **1** has been attempted twice (A.9). The first attempt was an 1:1 NMR scale reaction of **1** and $Pd(OAc)_2$ in benzene-d_6, but the NMR showed no signals likely due to the lack of solubility in **1**. The second attempt was still 1:1 of **1** and $Pd(OAc)_2$ but in toluene. $Pd(OAc)_2$ was very soluble in toluene, but **1** was not as soluble and could not fully dissolve when mixed. The NMR in toluene showed no signals which could be from Ru(II) not being completely soluble. Changing the solvent, temperature, or source of Pd(II) could change the solubility of this coordination in the future.

The synthesis of a Co(III) complex of [$Cp^*Co(PMe_3)(C_2$-2-py$)_2$] (**2**) was also attempted (A.7, A.8). Late transition metal complexes have been known to coordinate to electron-withdrawing ligands, and Co was chosen to replace Ru because Co is an Earth-abundant metal.[5] Additionally, the ionic radii of Co(III) is similar to the known Ti(IV) complex (Figure 11). Their similar electronics is important because [$Cp^*_2Ti(C_2$-2-py$)_2$] is known to coordinate to $Pd(Cl)_2$ and so [$Cp^*Co(PMe_3)(C_2$-2-py$)_2$] is likely to coordinate to $Pd(OAc)_2$.[17] The low spin d^6 characterization of Co(III) has the potential to behave like the Ru(II) if not better since Co(III) has a reduced π-basicity. The structure with Co(III) is more flexible to position the nitrogens on

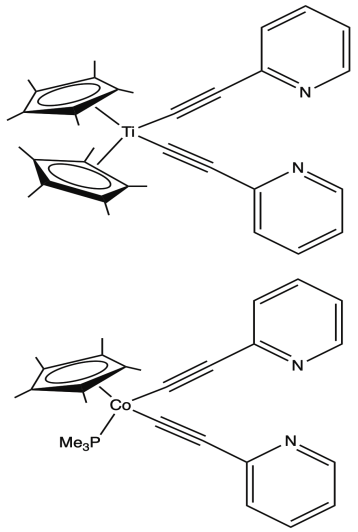

*Figure 11 Comparing [$Cp^*_2Ti(C_2$-2-py)$_2$] to **2***

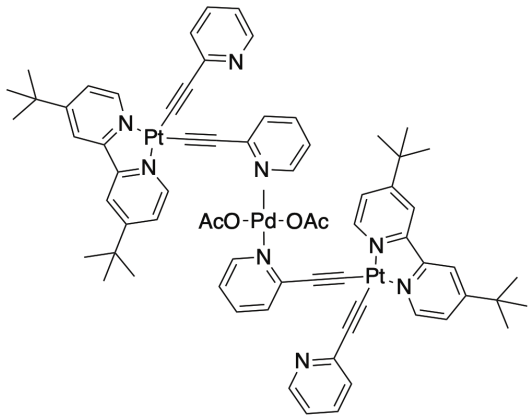

Figure 12 [^{t}bpyPt(C_2-2-py)$_2$Pd(OAc)$_2$]

pyridine to face each other and force a *trans*-bidentate ligand. In addition, this lack of π-back-bonding is ideal because it has been reported that an electron-rich Pt(II) from [^{t}bpyPt(C_2-2-py)$_2$] was unable to coordinate $Pd(OAc)_2$ to both nitrogens in a *trans* manner (Figure 12).[11] There was not enough flexibility for the reaction to coordinate as planned, and the Ru(II) complex could produce similar results. Because of these reasons, the Co(III) complex was attempted. The reaction was set up similarly to the synthesis of **1** with attempts using ^{n}BuLi and LiHMDS as the bases (Scheme 4).

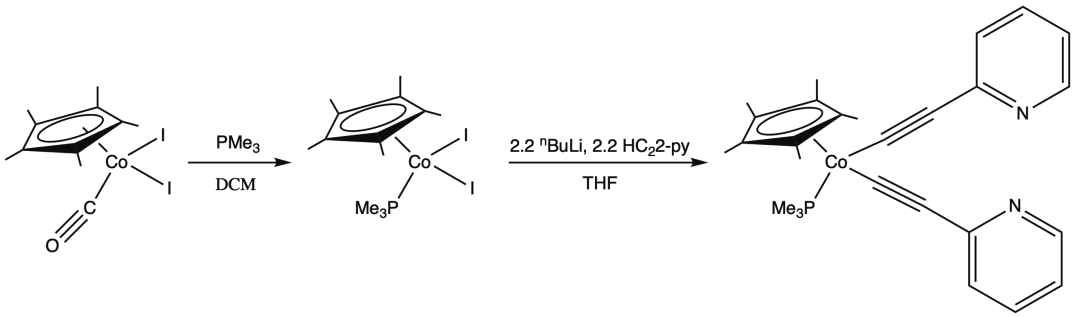

*Scheme 4 Synthesis of **2***

The NMR gave inconclusive results which suggested the Co(III) complex could have reduced to Co(II) based on no observed signal in the NMR. Future work using different solvents and bases or changing the temperature can be investigated.

4. Conclusions

To summarize, the best experiment to synthesize of [(*p*-cym)Ru(PMe_3)(C_2-2py)$_2$] **1** was using LiHMDS with a 0.9901 M 2-HC_2py in THF standard at room temperature inside the glovebox. This was a reproducible experiment with yields as high as 42.6 %. The retained mirror symmetry in the NMR of **1** along with the phosphorus shift at 15 ppm when 2-HC_2py was added confirmed the synthesis of **1.** Future work with **1** involves new purification techniques and obtaining a crystal structure. Replacing Ru(II) with Co(III) for [Cp^*Co(PMe_3)(C_2-2-py)$_2$] **2** can also be further investigated such as changing the base and temperature. Future experiments inserting a Pd(II) complex onto **1** involves changing the temperature, solvent, stoichiometric ratios, and source of Pd(II). If [(*p*-cym)Ru(PMe_3)(C_2-2-py)$_2$Pd(OAc)$_2$] can be made, studying the catalytic cycle on benzene will be the next step.

5. References

1. Webster-Gardiner, M. S.; Piszel, P. E.; Fu, R.; McKeown, B. A.; Nielsen, R. J.; Goddard, W. A., III; Gunnoe, T. B. *J. Mol. Catal.* **2017**, *426*, 381-388.
2. Comanescu, C. C.; Iluc, V. M. *Inorg. Chem.* **2014,** *53*, 8517-8528.
3. Wang, N; McCormick, T. M.; Ko, S.; Wang, S. *Euro. J. Inorg. Chem.* **2012**, 4463-4469.
4. Jung, M.; Suzaki, Y.; Saito, T.; Shimada, K.; Osakada, K. *Polyhedron* **2012,** *40*, 168-174.
5. Vieira N.C.; Pienkos J.A.; McMillen C.D.; Myers A.R.; Clay A.P.; Wagenknecht P.S. *Dalton Trans.,* **2017**, *46*, 15195.
6. Lee, J. P.; Hankins, M. J.; Riner, A. D.; Albu, T. V. *J. Coord. Chem.* **2016,** *69*, 20-38.
7. Touchard, D.; Dixneuf, P. H. *Coord. Chem. Rev.* **1998,** *178-180*, 409-429.
8. Menendez, C.; Morales, D.; Perez, K.; Riera, V. *Organometallics*. **2001**, *20*, 2775-2781.
9. WebElements. https://www.webelements.com (accessed November 2, 2020).
10. Szarek, P.; Witkowski, M.; Wozniak, A. P. *J. Phys. Chem. C* **2019,** *123*, 11572-11580.
11. Jaques, L. D.; McDarmont, S. L.; Smart, M. M.; McMillen, C. D.; Neglia, S. E.; Lee, J. P.; Pienkos, J. A. *Inorg. Chem. Comm.* **2020,** *112*, 107722.
12. Teo, B.K.; Xu Y.H.; Zhong B.Y.; He Y.K.; Chen, H.Y.; Qian W; Deng Y.J.; Zou Y.H. *Inorg. Chem.* **2001**, *40*, 6795.
13. Sugimoto, K.; Tanaka, Y.; Fujii, S.; Tada, T.; Kiguchi, M.; Akita, M. *Chem. Comm.* **2016**, *52*, 5796-5799.
14. Lu,W.; Chan, M.C.W.;Zhu,N.; Che C.; He Z. *Chem. Eur. J.* **2003**, *9*, 6155-6166.
15. Gottlieb, H. E.; Kotlyar, V.; Nudelman, A. *J. Org. Chem.* **1997,** *62*, 7512-7515.
16. Emmert, M. H.; Cook, A. K.; Xie, Y. J.; Sanford, M. S.. *Angew. Chem., Int. Ed.* **2011,** *50*, 9409-9412, S9409/1-S9409/34.
17. Vieira N.C.; Pienkos J.A.; McMillen C.D.; Myers A.R.; Clay A.P.; Wagenknecht P.S. *Dalton Trans.,* **2017**, 46, 15195.

Chapter 3: Computational Studies in the Design of a Highly Electron Deficient bis-Imine Ligand

1. Introduction

Many transition metal complexes rely on directing groups to promote selectivity for C-H bond activation, so functionalizing unactivated hydrocarbons is even more challenging to enforce. Reports show that electrophilic metal catalysts such as Pt(II), Hg(II), and Pd(II) can cleave the C-H bonds in hydrocarbons.[1] The mechanism follows an electrophilic substitution reaction (Scheme 1). The functionalization of a C-H bond is a novel method for converting

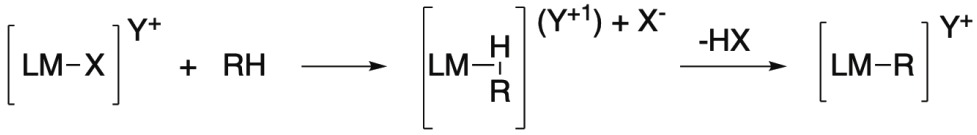

Scheme 1 Electrophilic Substitution Reaction

hydrocarbons to higher valued products. However, most of the electrophiles used need to operate in highly acidic conditions to attack the C-H bond such as with a silver salt, AgX where X = triflate, acetate, tetrafluoroborate, etc.[2,3] Over-oxidation is another challenge that remains from the electron-poor metal complexes. Although, the addition of electron-withdrawing groups can protect the complex from over-oxidizing.[1] For example, an electron-withdrawing bisulfate group protects oxidation when a Pt catalyst is used for activating methane in oleum to produce methylbisulfate.[4] The bisulfate group increases the activation barrier for electrophilic C-H activation.[4] In this chapter, the focus is to study electron-withdrawing ligands to see which ligand is most likely to assist an electrophilic catalyst to follow C-H activation on benzene.

Ir and Rh metal complexes have been known to activate the C-H bond in benzene.[5] A report by Gunnoe *et al.* showed that Rh(I) complexes bearing neutral bidentate nitrogen donors could act as a catalyst in H/D exchange for aromatics.[1,6] They found that this exchange follows an electrophilic arene substitution reaction for C-H activation. Several ligands were studied with differing electronic and steric properties, and *N,N′*-bis(pentafluorophenyl)-2,3-dimethyl-1,4-

diaza-1,3-butadiene was the most active catalyst. It was observed that the most electron-withdrawing ligands attached were the best to prevent the Rh(I) complex from oxidizing to Rh(III). Additionally, the more electrophilic the Rh metal center was, the better the reactivity. Using this research, imines with varying electronic character will be studied to see which ligand is the most electron-withdrawing and where the preferential binding sites are located.

This chapter is focused on computationally exploring the electron density in six imine ligands where **1** = *N,N'*-bis-(3,5-dimethylphenyl)-2,3-dimethyl-1,4-diaza-1,3-butadiene, **2** = *N,N′*-bis-(pentafluorophenyl)-2,3-dimethyl-1,4-diaza-1,3-butadiene, **3** = *N,N′*-bis-(4-pyridine)-2,3-dimethyl-1,4-diaza-1,3-butadiene, **4** = *N,N′*-bis-(2,3,5,6-tetrafluoripyridine)-2,3-dimethyl-1,4-diaza-1,3-butadiene, **5** = *N,N′*-bis-(2-pyridine)-2,3-dimethyl-1,4-diaza-1,3-butadiene, and **6** = *N,N′*-bis-(3,5-dimethylphenyl)-(2-pyridine)-2,3-dimethyl-1,4-diaza-1,3-butadiene (Figure 1). Both **1** and **2** were active precursors to the Rh(I) catalyst for H/D exchange between benzene and trifluoroacetic-d_1 acid, and **2** had the highest turnover (TO) of 140 and highest turnover frequency (TOF) 9.7 x 10^{-3} s^{-1}.[1] Placing a nitrogen on **3** should make the compound more electron-withdrawing than **1** so the energy barrier for C-H activation should be decreased. Replacing a fluorine with a nitrogen in **4** should make the ligand more electron poor than **2**.

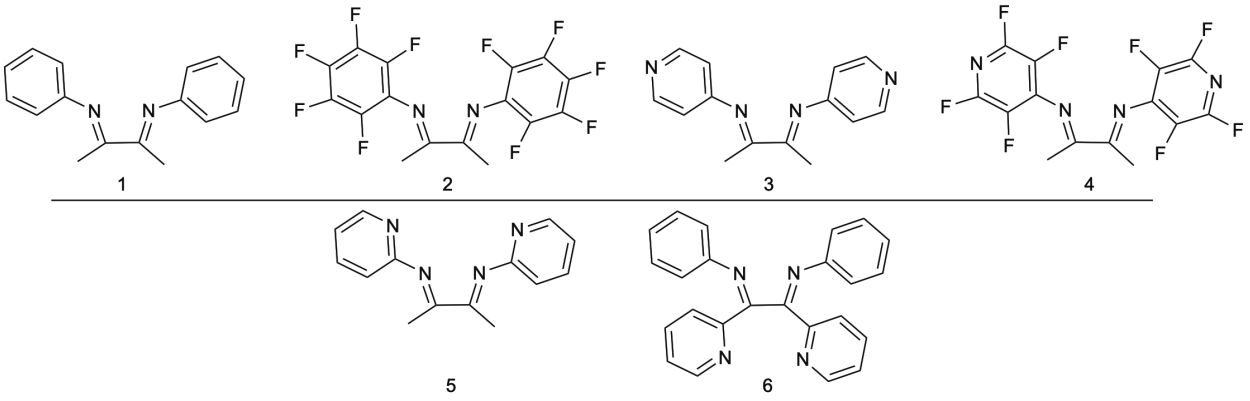

Figure 1 Six Imine Ligands for DFT Calculations

Compounds **5** and **6** were chosen to see the preferential site the metal would likely coordinate to given the opportunity for both sites to bind as a bidentate ligand.

To summarize, the first four structures will compare the effect of electron-withdrawing groups added to the complex. The last two structures will be evaluated to see where the electron density goes if both the imine and pyridine nitrogen has the potential to form a bidentate ligand. The density functional theory (DFT) calculations will suggest the proposed pathway for catalytic C-H activation.

2. Experimental

2.1 Measurements

All geometries were optimized to a minimum using Gaussian 16 software employing the B3LYP functional. For all atoms of the ligand, the basis set of 6-311G with a d-orbital polarization function was employed.[7-9] The electron density from Total Self-Consistent Field (SCF) density was mapped with electrostatic potential (ESP) at surface points only. All energies include a contribution for zero-point energies and free energies were computed at 298.15 K and 1 atm.

3. Results and Discussion

The computed zero-point inclusive energies of the ligands are reported below in Hartrees. These energies were summarized in the log output file of the optimization and frequency calculation for each compound (Table 1). Note, both **1** and **2** can bind to Rh(I) and when ethylene is coordinated are effective in promoting C-H activation.[1]

Table 1: Electronic Energy (EE) + Zero-point Energy (ZPE) Contribution (Hartree)	
1	**-728.699**
2	**-1720.989**
3	**-760.791**
4	**-1554.978**
5	**-760.800**
6	**-1144.239**

The structures were built in the *cis* conformation, but optimizing the geometry put the compounds in *trans* since this is the lowest energy conformation of the ligands. However, when the ligands coordinate to the metal center, the structure will rotate back to *cis* since both imine nitrogens coordinate to the metal center. Future computational work will be in forcing the *cis* geometry during the optimization calculations. In the check file, the highest occupied molecular orbital (HOMO) was generated through a new cube and the surface was mapped for each ligand. In addition, the total electron density was mapped with the electrostatic potential (ESP) at the surface points to show the electron density of the ligands. The ESP colors are scaled red to blue with red being electron-rich, green being neutral, and blue being electron-poor. Comparing the HOMO and ESP trends of each compound show how the nucleophilicity of the imine nitrogen changes as the number of electron-withdrawing groups changes.

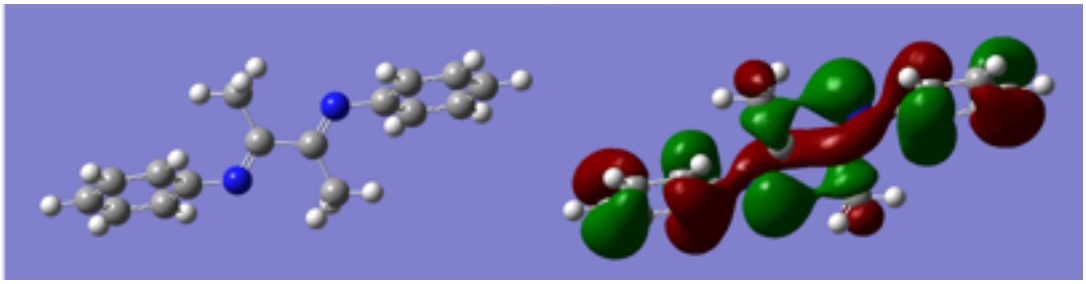

*Figure 2 HOMO of **1***

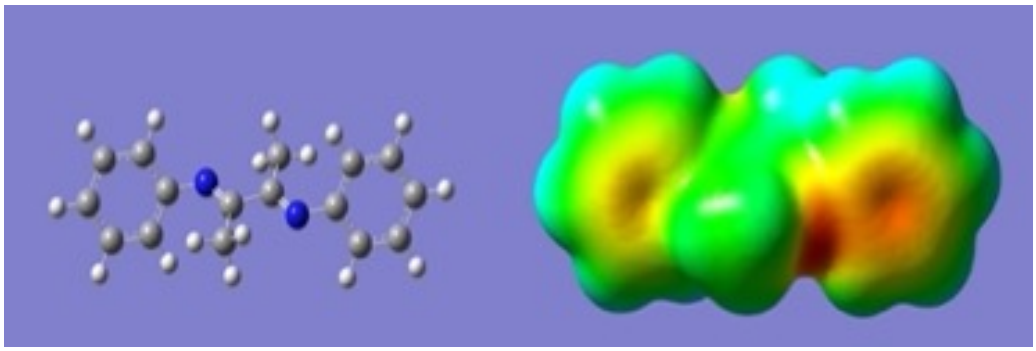

*Figure 3 ESP of **1***

Compound **1** has been reported as an active catalytic precursor for C-H activation on benzene.[1] The HOMO shows there is pi-bonding interaction on the phenyl rings along with ligand lone pair characterization on the imine nitrogen, and the localization is balanced between both parts (Figure 2). The ESP map shows the electron rich area to be at the imine nitrogen (Figure 3). Since the red area on the right side is faced down like the imine nitrogen in the structure beside it, this is likely the sp^2 hybridized lone pair. Overall, **1** is fairly neutral with electron withdrawing ends and an electron rich region at the imine to bind to a metal. The ESP map highlights the observation by Gunnoe *et al.* that electron withdrawing ligands are effective catalytic precursors for C-H activation since **1** was a successful ligand.[1]

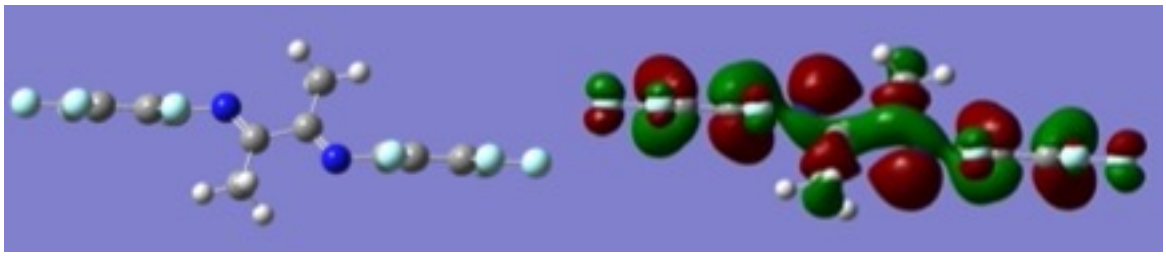

*Figure 4 HOMO of **2***

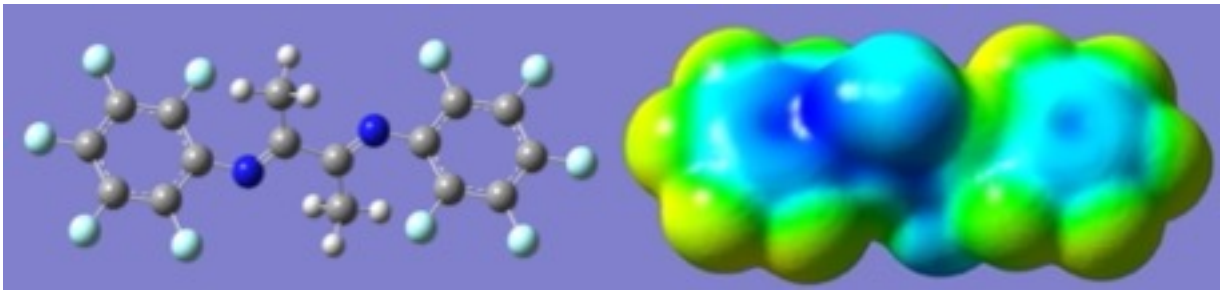

*Figure 5 ESP of **2***

Compound **2** was found to be the best catalytic precursor for C-H activation, and this ligand is very electron poor.[1] The HOMO shows there is pi-bonding interaction on the phenyl rings along with ligand lone pair characterization on the imine nitrogen, and the localization is more on the imine nitrogen than aromatics (Figure 4). The ESP map shows the entire ligand is electron poor, even at the imine, which changed from red to green (Figure 5). The electron-withdrawing fluorine groups pulled the electron density away from the imine nitrogen. Compared to **1**, adding the electron-withdrawing substituents (fluorines) onto the aromatic ring in **2** significantly impacts the electron density on the imine nitrogen. In **1**, the imine nitrogen is still electron rich, but in **2** the imine nitrogen is very electron poor. Since ligand **2** had the highest TO for catalytic activity on benzene, an overall electron poor ligand is worth noting for future ligands.[1]

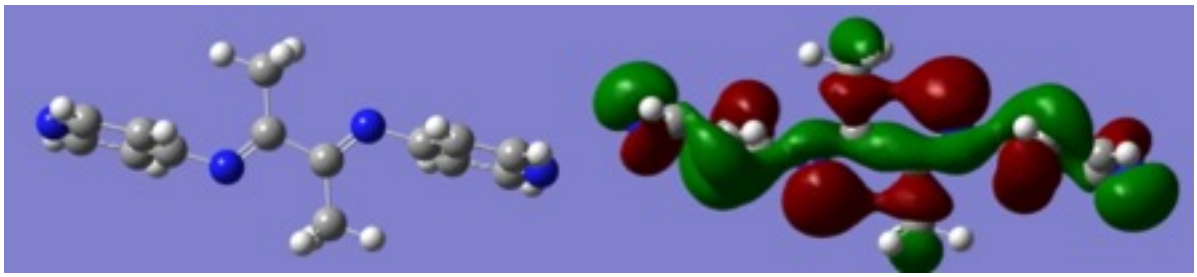

*Figure 6 HOMO of **3***

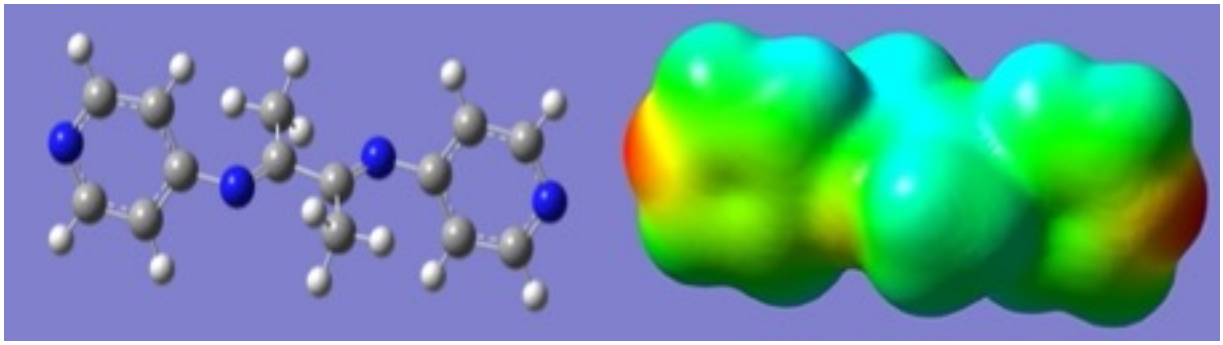

*Figure 7 ESP of **3***

The next compounds (**3** and **4**) contain *para*-pyridine rings instead of aromatic rings like in **1** and **2** to see if this change makes the ligand more electron-withdrawing. The HOMO in **3** shows there is pi-bonding interaction on the pyridines along with ligand lone pair characterization on both the imine and pyridine nitrogen, and the localization is balanced between these parts (Figure 6). The ESP map in **3** shows the electron rich area to be at the nitrogen on the pyridine instead of the imine (Figure 7). Indeed, protonating the nitrogen in pyridine and optimizing the geometry changed the electron rich area to be on the imine nitrogen. From **3**, the ligand is fairly neutral and would likely bind to a metal in a monodentate mode since the pyridines are more electron rich than the imines.

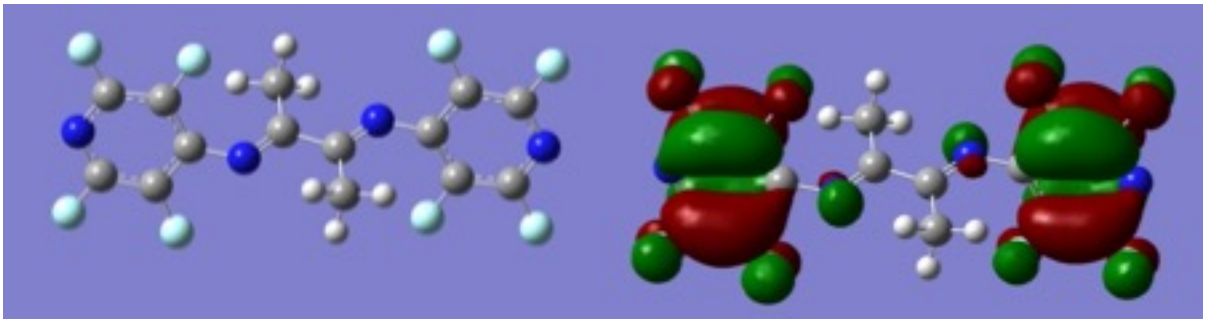

*Figure 8 HOMO of **4***

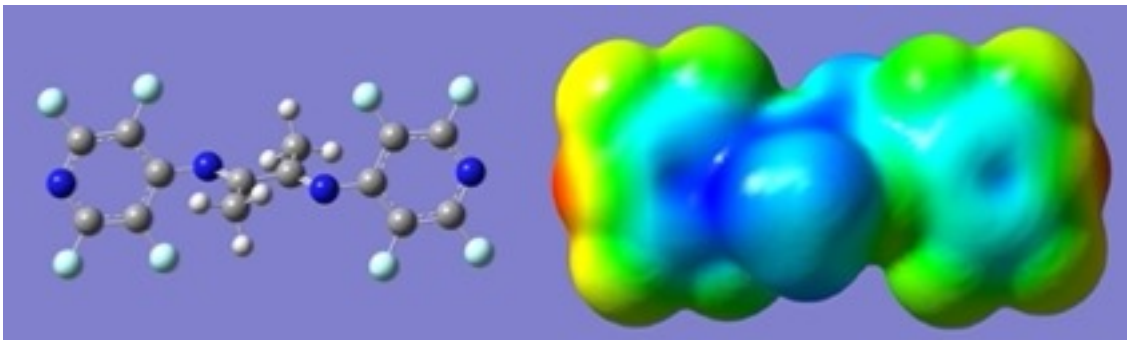

*Figure 9 ESP of **4***

Adding electron-withdrawing substituents to the pyridines (**4**) was analyzed next to see what happens to the electron density. Now, the HOMO shows there is mainly pi-bonding interaction on the pyridines along with small ligand lone pair characterization on the imine nitrogen (Figure 8). So, the localization is mainly on the aromatic rings. The ESP map shows the electron rich area to be at the nitrogen on the pyridine with poor electron density near the methyl groups (Figure 9). Since the pyridine is electron rich, it will likely bind to the metal there. Compared to **3**, the addition of the fluorines made the imines much more electron poor and the overall compound more electron poor since it is mainly blue and green in color.

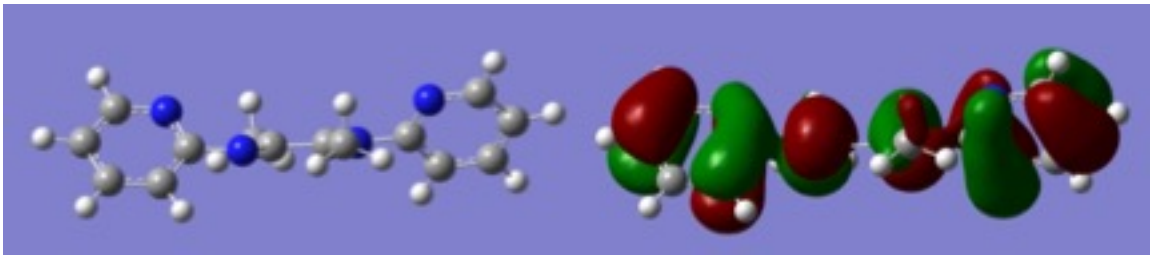

*Figure 10 HOMO of **5***

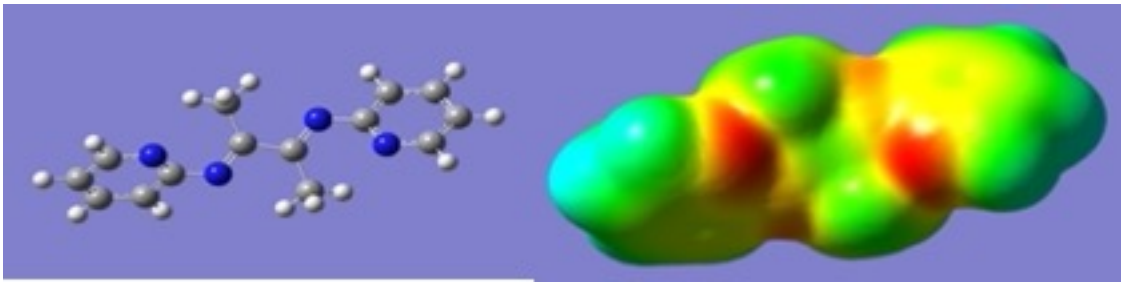

*Figure 11 ESP of **5***

The next couple of ligands (**5** and **6**) were analyzed to compare the binding preferences of the pyridine N to the imine N if both nitrogens were in a location to chelate. The HOMO in **5** shows there is pi-bonding interaction on the pyridine along with ligand lone pair characterization on the imine nitrogen, and the localization is balanced between both parts (Figure 10). The ESP map shows the electron rich area to be at the nitrogen on the pyridine and slightly on the imine nitrogen (Figure 11). Protonating the nitrogen on the pyridine moved the electron rich area to the imine. From **5**, the pyridines are likely to coordinate to the metal complex better than the imine in a bidentate fashion.

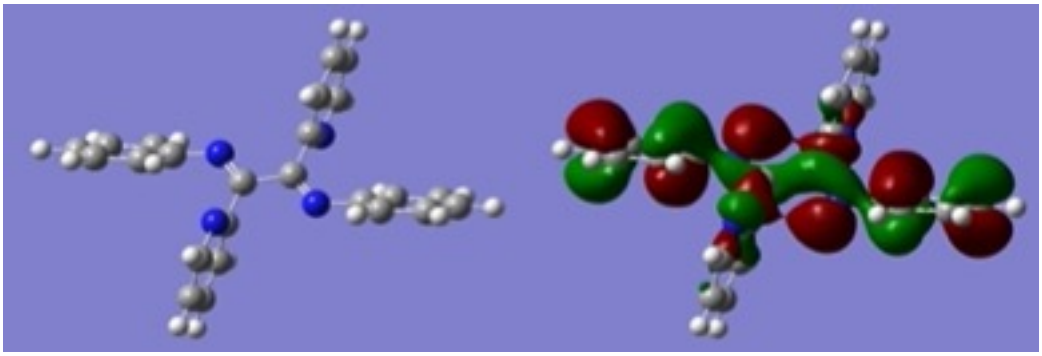

*Figure 12 HOMO of **6***

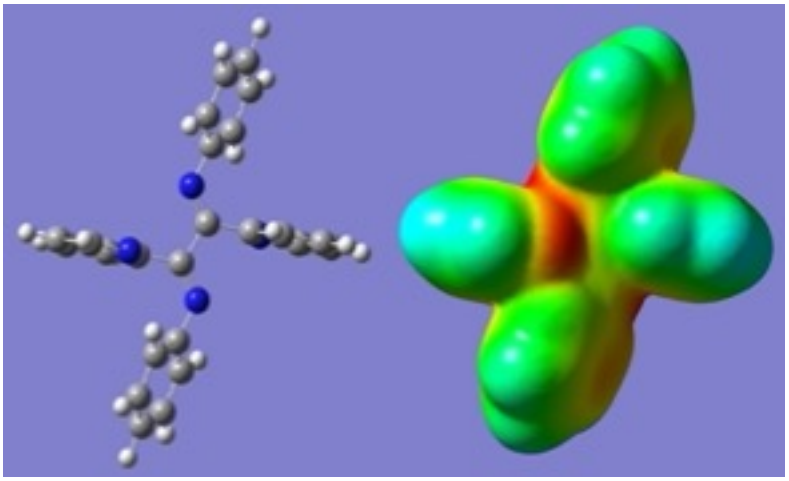

*Figure 13 ESP of **6***

In **6**, two *ortho*-pyridine rings were added in place of the methyl groups on the backbone of the diene. The HOMO shows there is pi-bonding interaction on the phenyl rings along with ligand lone pair characterization on the imine nitrogen, and the localization is balanced between both parts (Figure 12). There is not much character on the pyridine rings. The ESP map shows the electron rich area to be at the imine nitrogen and slightly on the pyridine nitrogen (Figure 13). Protonating the nitrogen on the pyridine moved the electron rich area to the phenyl groups, not the imine. Compared to **5**, the extra aromatic rings shifted the electron density in **6** to stay localized at the imine instead of the pyridine. So, ligand **6** is still more likely to chelate at the imine even though the pyridines have the ability as well.

4. Conclusions

Analyzing the electronic character of each ligand helped predict the likelihood of the ligand to bind to a metal center and facilitate a C-H functionalization reaction. The ligand **2** is known to promote C-H activation on a Rh(I) complex.[1] The ligand has five fluorine atoms attached to each aromatic ring that withdraw the electron density away from the imine nitrogens to produce an electron poor ligand. Ligand **4** was optimized based on the idea that replacing one fluorine group with a nitrogen by using pyridine would make the ligand more electron poor than **2**. However, the ESP map showed that the nitrogen on the pyridine was very electron rich compared to the imine nitrogens, and the ligand had mainly pi character localized on the rings. Even though complexes prefer to bind at two sites because of the chelate effect, based on the electronic character, ligand **4** would likely coordinate in a monodentate mode utilizing a pyridine nitrogen. Compound **4** also had an ESP range closer to the known complexes of **1** and **2**, so this ligand could be a good catalytic precursor for C-H activation. Interestingly, removing all the fluorine groups on the pyridine gave a more balanced localization of pi character on the rings and lone pair character on the imine nitrogen in **3**. The ESP map on **3** showed the electron richness on the nitrogen in the pyridine, but it is still possible for a metal to bind at the imine location based on the HOMO's localization character and chelate effect. Removing the nitrogen, and simply having two phenyl rings attached to the imine was examined in **1**. The HOMO localization was balanced at the aromatics and imine, and the ESP showed the imine nitrogen to be electron rich which increases the chances for the metal to bind at this area in a bidentate fashion. Ligands **5** and **6** were analyzed to see where the electron density goes if both the imine and pyridine nitrogen can be bidentate. In **5** and **6**, the HOMO localization was on both the imine ligand lone pair and the aromatics. However, in **5**, the pyridine nitrogen was slightly more

electron-rich than the imine nitrogen. And in **6**, the imine nitrogen was slightly more electron-rich than the pyridine nitrogen. This suggests that the addition of bulky aromatics can tune the imine nitrogen to be the electron rich area. Studying the electronic character of the six imine compounds gave insight on the most electron withdrawing ligands and the preferential binding modes. Future work involves analyzing compound **4** for an effective ligand in C-H activation.

5. References

1. Webster-Gardiner, M. S.; Piszel, P. E.; Fu, R.; McKeown, B. A.; Nielsen, R. J.; Goddard, W. A., III; Gunnoe, T. B. *J. Mol. Catal. A: Chem.* **2017,** *426*, 381-388.
2. Shilov, A. E.; Shul'pin, G. B. *Chem. Rev.* **1997,** *97*, 2879-2932.
3. Munz, D.; Webster-Gardiner, M.; Fu, G., Strassner, T.; Goddard, W. A., III; Gunnoe, T. B. *ACS Catal.* **2015**, *5*, 2985-2996.
4. Periana, R.A., Taube, D.J., Gamble, S., Taube, H., Satoh, T., Fujii, H. *Science*, **1998**, *280*, 560-564.
5. Tenn, W.J.; Conley, B.L.; Bischof, S.M.; Periana, R.A. *J. Organomet. Chem.* **2011**, *696*, 511-558.
6. Vaughan, B. A.; Khani, S. K.; Gary, J. B.; Kammert, J. D.; Webster-Gardiner, M. S.; McKeown, B. A.; Davis, R. J.; Cundari, T. R.; Gunnoe, T. B. *J. Am. Chem. Soc.* **2017,** *139*, 1485-1498.
7. Raghavachari, K.; Binkley, J.S.; Seeger, R.; Pople, J.A. *J. Chem. Phys.* **1980**, *72*, 650-654.
8. Hay, P.J. *J. Chem. Phys.* **1977**, *66*, 4377-4384.
9. Raghavachari, K.; Trucks, G.W. *J. Chem. Phys.* **1989**, *91*, 1062-1065.

Appendix

Experimental reaction attempts

A.1 Attempted Preparation of [(*p*-cym)Ru(PMe_3)(C_2-Ph)$_2$] using ^{n}BuLi

To an oven-dried 100 mL Schlenk flask, PhC_2H (58.44 μL, 0.572 mmol) and THF (10 mL) was added on the Schlenk line using a microliter syringe and canula needle. The flask was placed on an acetone/ N_2 (l) bath to -78 °C for 10 min. ^{n}BuLi (0.36 mL, 0.572 mmol) was added and the flask was left in the bath for another 10 min then cooled to room temperature for 0.5 h. [(*p*-cym)Ru(PMe_3)($Cl)_2$] (0.1094 g, 0.286 mmol) was added to the brown peach solution and left to stir for 24 h. The homogeneous dark brown solution was transferred into the glovebox to remove solvent *in vacuo*. A sample of the brown powder was dissolved in $CDCl_3$ to run an NMR. The desired compound was not made.

A.2 Attempted Preparation of [(*p*-cym)Ru(PMe_3)(C_2-Ph)$_2$] using $AgNO_3$

$AgNO_3$ (1.0281 g, 6.000 mmol) was dissolved in MeCN (70 mL) in a 100 mL oven-dried Erlenmeyer flask. PhC_2H (2.03 mL, 18.0 mmol) and NEt_3 (2.56 mL, 18.0 mmol) was added to the flask in 0.5 mL portions with vigorous stirring to turn the clear solution a milky white. The flask was left to stir for 48 h. The white precipitate inside the flask was collected by vacuum filtration and rinsed with MeCN (3 x 50 mL) and MeOH (3 x 50 mL). An NMR sample of the dried solid was attempted using DMSO but the product was completely insoluble, but the compound of AgC_2Ph was assumed to be made. The AgC_2Ph solid (0.1070 g, 0.523 mmol) and [(*p*-cym)Ru(PMe_3)($Cl)_2$] (0.0518 g, 0.131 mmol) was added to a clean 100 mL round bottom flask followed by DCM (20 mL) to make a milky orange soln. Foil was wrapped around the flask and this was left to stir for 2 h. The heterogeneous brown/ lavender solution was filtered through celite with DCM. An NMR sample was taken in DMSO of the product recovered but only starting material showed up.

A.3 Attempted Preparation of (*p*-cym)Ru(PMe_3)(C_2-Ph)$_2$] using AgOTf

To an oven-dried 100 mL Schlenk flask, [(*p*-cym)Ru(PMe_3)($Cl)_2$] (0.0492 g, 0.129 mmol), AgOTf (0.1340 g, 0.512 mmol), and DCM (10 mL) were added inside the glovebox and left to stir for 2 h as a heterogeneous orange solution. In another oven-dried 100 mL Schlenk flask on the Schlenk line, PhC_2H (35.33 µL, 0.322 mmol) through a microsyringe and THF (10 mL) was added with a canula needle. This flask was placed in an acetone/ N_2 (l) bath at -78 °C for 10 min, then ^{n}BuLi (0.20 mL, 0.322 mmol) was added for 15 min. The flask was taken off the bath and left to cool to room temperature for 1 h with a pale-yellow appearance. The reaction in the glovebox was filtered through celite after 2 h of stirring and the filtrate was transferred to a new oven-dried 100 mL Schlenk flask and placed under vacuum to remove the DCM solvent. The dried powder inside the Schlenk flask was taken outside the glovebox and placed on the Schlenk line where the flask containing PhC_2 was transferred to the Ru(II) flask from a canula needle. The homogeneous brown solution was left to stir for 16 h then placed back inside the glovebox to remove the THF solvent under vacuum. The brown residue was dissolved in DCM and filtered through celite and the product filtrate was placed under vacuum to remove the solvent. An NMR sample of the brown solid was dissolved in $CDCl_3$ but the **1**'s peaks were missing so the compound was not made.

A.4 Attempted Preparation of [(*p*-cym)Ru(PMe_3)(C_2-2-py)$_2$] using ^{n}BuLi

Inside the glovebox, 0.9901 M of 2-HC_2py in THF (0.56 mL, 0.549 mmol) followed by more THF (15 mL) was added to an oven-dried 100 mL Schlenk flask. The flask was placed on the Schlenk line under a purge of N_2 and cooled to -78 °C in an acetone/ N_2 (l) bath. After 10 min, ^{n}BuLi (0.21 mL, 0.549 mmol) was added to the pale-yellow solution. The solution was left in the bath for 15 min before removing the cold bath to warm to room temperature for 10 min.

The solution was dark brown and [(*p*-cym)Ru(PMe_3)$(Cl)_2$] (0.1040 g, 0.262 mmol) was added and left to stir for 4 h. The dark brown solution was brought inside the glovebox and to remove THF *in vacuo*. The black/brown powder was taken outside the glovebox for a silica gel purification with 5% NEt_3 in DCM. The product filtrate was placed on the rotary evaporator to until there was minimal solvent. Hexanes were added to the flask but removed *in vacuo* since a product did not precipitate out. The dried brown powder (0.0480 g, 34.2%) was taken to run an NMR in $CDCl_3$ and the desired product was formed, but not consistently.

A.5 Attempted Preparation of [(*p*-cym)Ru(PMe_3)$(C_2$-2-py$)_2$] using KPF_6

Inside the glovebox, [(*p*-cym)Ru(PMe_3)$(Cl)_2$ (0.1007 g, 0.262 mmol) and KPF_6 (0.142 g, 0.785 mmol) were added to an oven-dried 50 mL Schlenk flask followed by DCM (10 mL). The solution was homogenous red then the 0.9901 M standard of 2-HC_2py in THF (0.80 mL, 0.785 mmol) turned it darker and this flask was placed on the Schlenk line to add NEt_3 (0.51 mL, 1.43 mmol). Foil was wrapped around the flask and the solution was left to stir for 48 h. The flask was brought back inside the glove box to remove solvent *in vacuo.* An NMR sample of the brown residue was dissolved in $CDCl_3$ and the desired product was not made.

A.6 Attempted Preparation of [(*p*-cym)Ru(PMe_3)$(C_2$-2-py$)_2$] using CuI

Inside the glovebox, [(*p*-cym)Ru(PMe_3)$(Cl)_2$ (0.1068 g, 0.262 mmol) was added to an oven-dried 100 mL Schlenk flask followed by DCM (15 mL). The 0.9901 M of 2-HC_2py in THF (0.65 mL, 0.786 mmol) was added. The homogenous dark red/brown solution was brought to the Schlenk flask. CuI (0.0036 g, 0.026 mmol) followed by $NH(iPr)_2$ (2.45 mL, 21.5 mmol) was added under a strong purge of nitrogen. The brown/red solution was covered in foil and left to stir for 24 h. The dark brown solution was purified on a Al_2CO_3 column with DCM. The

product filtrate was placed on the rotary evaporator to dissolve solvent. An NMR sample in $CDCl_3$ was taken but the desired product was not made.

A.7 Attempted Preparation of [$Cp^*Co(PMe_3)(C_2$-2-py$)_2$] (**2**) using LiHMDS

An oven-dried 50 mL Schlenk flask was brought inside the glovebox and a 0.9901 M of 2-HC_2py in THF (0.21 mL, 0.21 mmol) followed by THF (5 mL) was added. LiHMDS (0.0351 g, 0.21 mmol) was added and left to stir for 0.5 h. The heterogeneous yellow/brown solution turned dark brown when [(Cp^*)$Co(PMe_3)(I)_2$] (0.0503 g, 0.0954 mmol) was added. This stirred for 4 h. THF was removed *in vacuo* and the solid was rinsed with hexanes through vacuum filtration. The brown powder was taken to run an NMR sample in $CDCl_3$, but only impurities were present.

A.8 Attempted Preparation of [$Cp^*Co(PMe_3)(C_2$-2-py$)_2$] (**2**) using ^{n}BuLi

An oven-dried 100 mL Schlenk flask was brought inside the glovebox to add 0.9901 M of 2-HC_2py in THF (0.21 mL, 0.21 mmol) followed by THF (5 mL). The flask was capped and brought to the Schlenk line under a purge of N_2 and cooled to -78 °C in an acetone/ N_2 (l) bath. After 10 min, ^{n}BuLi (0.08 mL, 0.21 mmol) was added to the pale-yellow solution. The solution was left in the bath for 15 min before removing the cold bath to warm to room temperature for 10 min. The solution turned dark yellow/brown. [(Cp^*)$Co(PMe_3)(I)_2$] (0.0508 g, 0.0954 mmol) was added to the solution under a purge of N_2. After 4 h of stirring, it was a dark brown homogeneous solution. THF was removed from the rotary evaporator leaving a dark brown gooey residue. Desired product was not made based on the NMR sample dissolved in $CDCl_3$.

A.9 Attempted Preparation of [(*p*-cym)$Ru(PMe_3)(C_2$-2-py$)_2Pd(OAc)_2$]

An oven-dried 25 mL Schlenk flask was brought inside the glovebox and [(*p*-cym)$Ru(PMe_3)(C_2$-2-py$)_2$] (0.070 g, 0.136 mol) and $Pd(OAc)_2$ (0.0316 g, 0.136 mol) were

added. Toluene (5 mL) was poured in to produce a dark brown soln. The $Pd(OAc)_2$ immediately dissolved in solution. After 20 h of stirring, toluene was removed *in vacuo* inside the glovebox leaving a brown solid. The solid was washed with diethyl ether and placed under vacuum filtration. The brown solid was dissolved in $CDCl_3$ to run a concentrated NMR sample, but the desired product was not made.